BIFURCATION PATTERNS IN HOMOGENEOUS AREA-PRESERVING PIECEWISE-LINEAR MAPS

ABSTRACT. The dynamical behavior of a family of planar continuous piecewise linear maps with two zones is analyzed. Assuming homogeneity and preservation of areas we obtain a canonical form with only two parameters: the traces of the two matrices defining the map. It is shown the existence of sausage-like structures made by lobes linked at the nodes of a nonuniform grid in the parameter plane. In each one of these structures, called resonance regions, the rotation number of the associated circle map is a given rational number. The boundary of the lobes and a significant inner partition line are studied with the help of some Fibonacci polynomials.

1. INTRODUCTION

In this paper, the dynamical behavior of some two-dimensional continuous piecewise-linear maps with two zones is analyzed. Under our assumptions of homogeneity and area preservation, we get a reduced canonical form where the only two parameters are the traces of the two matrices defining the map.

We start by assuming that the discrete system to be studied is of the form

$$\mathbf{x}_{n+1} = \mathbf{F}(\mathbf{x}_n) = \begin{cases} A^-\mathbf{x}_n + \mathbf{b}^- & \text{if } \mathbf{x}_n \in \Sigma^-, \\ A^+\mathbf{x}_n + \mathbf{b}^+ & \text{if } \mathbf{x}_n \in \Sigma^+, \end{cases} \tag{1}$$

where $\mathbf{x}_n = (x_n, y_n)^T$, $A^- = (a_{ij}^-)$ and $A^+ = (a_{ij}^+)$ are 2×2 constant matrices, $\mathbf{b}^- = (b_1^-, b_2^-)^T$ and $\mathbf{b}^+ = (b_1^+, b_2^+)^T$ are constant vectors of $\mathbb{R}^2$, and the linearity regions in the phase plane are the left and the right half-planes

$$\Sigma^- = \{\mathbf{x} = (x, y) \colon x < 0\}, \quad \Sigma^+ = \{\mathbf{x} = (x, y) \colon x > 0\},$$

so that the line $\Sigma = \{\mathbf{x} = (x, y) \colon x = 0\}$ is the *switching* line.

2010 *Mathematics Subject Classification.* 34C05, 34C07, 37G15.

Key words and phrases. Piecewise linear maps, Bifurcations, Area preserving maps.

In principle, these systems have twelve parameters. However, if we take into account the continuity along the line Σ, then the condition

$$A^- \begin{pmatrix} 0 \\ y \end{pmatrix} + \mathbf{b}^- = A^+ \begin{pmatrix} 0 \\ y \end{pmatrix} + \mathbf{b}^+,$$

holds for all $y \in \mathbb{R}$, so that both matrices $A^\pm$ share the second column and the vectors $\mathbf{b}^\pm$ coincide, that is

(2)
$$A^- = \begin{pmatrix} a_{11}^- & a_{12} \\ a_{21}^- & a_{22} \end{pmatrix}, A^+ = \begin{pmatrix} a_{11}^+ & a_{12} \\ a_{21}^+ & a_{22} \end{pmatrix}, \mathbf{b} = \mathbf{b}^- = \mathbf{b}^+ = \begin{pmatrix} b_1 \\ b_2 \end{pmatrix}$$

and so our systems have eight parameters.

When $a_{12} = 0$, the dynamics of the first variable is uncoupled from the dynamics of the second one and so our system would not be a proper two-dimensional system. This case will not be considered, assuming generically that $a_{12} \neq 0$.

In order to study the dynamical behavior of system (1) it is very convenient to find a canonical form with fewer parameters. To this end, we make the linear change of variables

$$\tilde{\mathbf{x}} = h(\mathbf{x}) = \begin{pmatrix} 1 & 0 \\ a_{22} & -a_{12} \end{pmatrix} \mathbf{x} - \begin{pmatrix} 0 \\ b_1 \end{pmatrix},$$

which keeps invariable both the line Σ and the half planes $\Sigma^\pm$. After dropping tildes, system (1)-(2) is transformed into the system

$$\mathbf{x}_{n+1} = \begin{pmatrix} T^\pm & -1 \\ D^\pm & 0 \end{pmatrix} \mathbf{x}_n + \begin{pmatrix} 0 \\ b \end{pmatrix} \quad \text{for} \quad \pm x_n \geqslant 0, \tag{3}$$

where $b = b_1(a_{22} - 1) - a_{12}b_2$ and we have denoted by T^- and T^+ and by D^- and D^+ the traces and determinant of matrices A^- and A^+, respectively. If $b \neq 0$, the additional scaling $\mathbf{x} \to b\mathbf{x}$ allows us to state the following result.

Proposition 1.1. *If $a_{12} \neq 0$ in system (1)-(2), then system (1)-(2) is linearly conjugated to the canonical form*

$$\begin{aligned} \mathbf{x}_{n+1} &= \begin{pmatrix} T^- & -1 \\ D^- & 0 \end{pmatrix} \mathbf{x}_n + \begin{pmatrix} 0 \\ m \end{pmatrix} \quad \textit{if } \mathbf{x}_n \in \Sigma^- \bigcup \Sigma, \\ \mathbf{x}_{n+1} &= \begin{pmatrix} T^+ & -1 \\ D^+ & 0 \end{pmatrix} \mathbf{x}_n + \begin{pmatrix} 0 \\ m \end{pmatrix} \quad \textit{if } \mathbf{x}_n \in \Sigma^+, \end{aligned} \tag{4}$$

where either $m = 0$ (homogeneous case) or $m = 1$ (non-homogeneous case).

The relevance of the above canonical form is multiple. On the one hand, it captures the celebrated Lozi system [13], which is considered the simplest dissipative piecewise linear map with chaotic solutions, namely

$$\begin{aligned} x_{n+1} &= 1 - \alpha|x_n| + y_n, \\ y_{n+1} &= \beta x_n, \end{aligned}$$

which represents the piecewise linear version of the Henon map [7]. Efectively, the change of variables $u_n = -x_n, v_n = 1+y_n$ put the system in the form (4) with $m = 1, D^+ = D^- = -\beta$ and $T^+ = -T^- = \alpha$. On the other hand, the canonical form (4) is equivalent to the prototype piecewise linear form introduced by Nusse and Yorke in [14] where the gave a piecewise affine approximation with only five parameters for a piecewise defined map. Note that while in [3] and [14] the bifurcation parameter is continuously varied in order to study the consequences of a border collision bifurcation, our canonical form emphasizes that the two only significant values to consider for the non-homogeneous term m are 0 and 1.

Here, we are not directly interested in the border-collision bifurcation, and following [10]-[12], we deal with the homogeneous case $m = 0$, relegating the non-homogeneous case $m = 1$ to future work. Moreover, we will pay attention only to the non-generic but important case of area-preserving maps, that is we will assume $D^+ = D^- = 1$, so that the system to be studied becomes,

$$\mathbf{x}_{n+1} = \mathbf{G}(\mathbf{x}_n) = \begin{cases} A(T_L)\mathbf{x}_n, & \text{if } \mathbf{x}_n \in \Sigma^- \cup \Sigma, \\ A(T_R)\mathbf{x}_n, & \text{if } \mathbf{x}_n \in \Sigma^+, \end{cases} \tag{5}$$

where T_R and T_L are the traces of the right and left matrices and

$$A(T) = \begin{pmatrix} T & -1 \\ 1 & 0 \end{pmatrix}.$$

Although the map has only two pieces and two parameters, the study of its dynamical behavior is far from being trivial because the orbits corresponding to each initial point cannot be generically expressed in closed form. In fact, we obtain the n iterate of a point $\mathbf{x}_0 = (x_0, y_0)^T$ as

$$\mathbf{x}_n = \mathbf{G}^n(\mathbf{x}_0) = A_n A_{n-1} \dots A_2 A_1 \mathbf{x}_0 = A_n \mathbf{x}_{n-1}. \tag{6}$$

where A_1 is $A(T_L)$ or $A(T_R)$ according to (5), and for $k \geqslant 2$ the matrix A_k is either $A(T_L)$ or $A(T_R)$ depending on the sign of $x_{k-1} = \mathbf{e}_1^T \mathbf{x}_{k-1}$, where $\mathbf{e}_1$ is the first canonical vector. With such a choice, we will say that the product of matrices appearing in (6) is admisible for the initial point $\mathbf{x}_0$. In any case, if for some $\mathbf{x}_0$ and $0 \leqslant k \leqslant n-1$, we

have $\mathbf{x}_k \in \Sigma$, that is $x_k = 0$, then two different products of matrices at least are admissible for such initial value $\mathbf{x}_0$. As it is remarked in [2], an explicit description of which products of matrices are admissible and which are not, for every case, remains an open problem.

From (5), it is immediately obtained that $\mathbf{G}(\lambda\mathbf{x}) = \lambda\mathbf{G}(\mathbf{x})$ for all $\lambda > 0$, and so we see that any ray starting at the origin is mapped into another ray also starting at the origin. Therefore, we can define a circle map $\mathcal{S}$ associating the intersection points of both rays with the unit circle. This fact allows us to split the dynamical behavior of the planar map in two different dynamics: the map $\mathcal{S}$ defined on the unit circle plus another dynamical system giving account of the expansion or contraction along the different rays. We will pay special attention to the dynamics generated by the circle map $\mathcal{S}$.

In our case, the maps $\mathbf{G}$ and $\mathcal{S}$ are reversible with respect to the diagonal of the first quadrant, see Proposition 2.1, so their periodic orbits either are symmetrical with respect to the reversibility axis or they appear in symmetric pairs with opposite stability.

Family (5) has been already studied in a series of papers by Lagarias and Rains, see [10], [11] and [12], where many properties of periodic behavior were obtained, see for instance Theorem 2.4 below. Also, parametrical regions with fixed rational rotation number (for certain rationals) were reported but not completely described. The main goal of this paper is to contribute in the description of some of these parametric regions giving both new qualitative and quantitative information.

The regions in the parameter space with a non-empty interior having a constant rational rotation number are called resonance tongues due to their typical shape. These resonance tongues can shrink into single points, usually called shrinking points, leading to a sausage-like structure first described for piecewise linear maps in [16]. In our paper, some specific properties of resonance tongues in the parameter plane determined by the two traces T_L, T_R are considered. We also show that the map $\mathcal{S}$ with parameters belonging to the interior of a resonance tongue has one pair of mutually symmetrical periodic orbits with opposite stability. At the boundary of a resonance region, we will see that these two periodic orbits collapse in a smooth saddle node bifurcation of periodic orbits, without involving any transition of the points in the orbit through the switching line in the phase plane.

We remark that in the celebrated work [15], the authors studied the non-homogeneous case of our family where the resonance tongues behave in a rather different way. In the quoted paper, the boundaries of the analyzed resonance regions correspond either to a loss of stability

of the associated periodic solutions or to a collision of one point of the orbit with the switching manifold. Therefore, the periodic orbits living in the resonance tongues analyzed in [15] disappear by means of a different mechanism from the ones studied in this paper. Additionally, we also provide explicit parametric values for some specific shrinking points and the local expansions for the boundaries of the associated resonance tongues. In some cases, the complete resonance boundaries are also provided. Before stating our main contributions, we review in next section some known preliminary results.

2. Preliminary results

Starting the study of the dynamics of system (5), it is worth noting that the origin is the only fixed point. In fact, the map $\mathbf{G}$ is a homeomorphism whose inverse is the map $\mathbf{G}^{-1}$ defined as follows,

$$\mathbf{x}_{n+1} = \mathbf{G}^{-1}(\mathbf{x}_n) = \begin{cases} A^{-1}(T_L)\mathbf{x}_n, & \text{if } y_n \leqslant 0, \\ A^{-1}(T_R)\mathbf{x}_n, & \text{if } y_n > 0, \end{cases} \tag{7}$$

where $\mathbf{x}_k = (x_k, y_k)$ and

$$A^{-1}(T) = \begin{pmatrix} 0 & 1 \\ -1 & T \end{pmatrix}.$$

Next, we consider two useful properties that allow us to reduce the number of different cases to be analyzed. Their proofs are direct and they will not be detailed.

Proposition 2.1. *The following statements hold for map* $\mathbf{G}$ *defined in* (5).

(a) *The map* $\mathbf{G}$ *is invariant under the change of variables and parameters*

$$(\mathbf{x}; T_L, T_R) \to (-\mathbf{x}; T_R, T_L), \tag{8}$$

that is, $\mathbf{G}(-\mathbf{x}) = -\mathbf{G}(\mathbf{x})|_{(T_L,T_R)\to(T_R,T_L)}$

(b) *The map* $\mathbf{G}$ *verifies the equality* $\mathbf{G}^{-1} = R \circ \mathbf{G} \circ R$, *where* R *is the involution defined as follows,*

$$\mathbf{x} \to R\mathbf{x} = \begin{pmatrix} 0 & 1 \\ 1 & 0 \end{pmatrix} \mathbf{x}.$$

That is, the map $\mathbf{G}$ *is reversible with respect to the involution* R.

From Proposition 2.1 (a), we see that the bifurcation diagram in the parameter plane (T_R, T_L) must be symmetrical with respect to the diagonal $T_R = T_L$. On the other hand, the reversibility shown in Proposition

2.1 (b) implies that the possible periodic orbits either appear in couples of mutually symmetrical orbits with opposite stabilities or they are self symmetrical with respect to the main diagonal in the phase plane.

To describe the associated circle map, the rays will be denoted as

$$\Pi_\theta = \{(x,y) : x = r\sin(2\pi\theta), y = -r\cos(2\pi\theta), 0 \leqslant \theta < 1, r \geqslant 0\}, \tag{9}$$

that is, the origin of angles is taken by using the negative y-axis as reference, the angle is defined modulo 2π, and the positive sense of angles is counter-clockwise.

The map $\mathbf{G}$ clearly induces a map on the unit circle S^1. Since any ray Π_{θ_0} is mapped by $\mathbf{G}$ into another ray Π_{θ_1}, we can define on S^1 the map $\mathcal{S} : S^1 \to S^1$ such that $\theta_1 = \mathcal{S}(\theta_0)$, that is $\Pi_{\theta_1} = \mathbf{G}(\Pi_{\theta_0})$. The following result, whose proof appears in Section 5, gives such a map and its natural lift. Along this paper, we consider the usual branch of $\tan^{-1}(\cdot)$ with values in the interval $(-\pi/2, \pi/2)$ and the branch of $\cot^{-1}(\cdot)$ taking values in the interval $(0, \pi)$.

Lemma 2.2. *The map $\mathcal{S} : S^1 \to S^1$ such that $\Pi_{\mathcal{S}(\theta)} = \mathbf{G}(\Pi_\theta)$ with $\mathbf{G}$ defined in* (5) *has the following explicit expression*

$$\mathcal{S}(\theta) = \begin{cases} 1/4, & \text{if } \theta = 0, \\ \frac{1}{2} - \frac{1}{2\pi}\tan^{-1}\left(T_R + \cot(2\pi\theta)\right), & \text{if } 0 < \theta < 1/2, \\ 3/4, & \text{if } \theta = 1/2, \\ 1 - \frac{1}{2\pi}\tan^{-1}\left(T_L + \cot(2\pi\theta)\right), & \text{if } 1/2 < \theta < \theta_{T_L}, \\ 0, & \text{if } \theta = \theta_{T_L}, \\ -\frac{1}{2\pi}\tan^{-1}\left(T_L + \cot(2\pi\theta)\right), & \text{if } \theta_{T_L} < \theta < 1, \end{cases} \tag{10}$$

where

$$\theta_{T_L} = \frac{1}{2} + \frac{1}{2\pi}\cot^{-1}(-T_L). \tag{11}$$

Furthermore, the corresponding lift $\mathcal{L}_\mathcal{S}$ of the the map $\mathcal{S}$ is as follows,

$$\mathcal{L}_\mathcal{S}(\theta) = \begin{cases} 1/4, & \text{if } \theta = 0, \\ \frac{1}{2} - \frac{1}{2\pi}\tan^{-1}\left(T_R + \cot(2\pi\theta)\right), & \text{if } 0 < \theta < 1/2, \\ 3/4, & \text{if } \theta = 1/2, \\ 1 - \frac{1}{2\pi}\tan^{-1}\left(T_L + \cot(2\pi\theta)\right), & \text{if } 1/2 < \theta < 1, \end{cases} \tag{12}$$

and its natural extension: $\mathcal{L}_\mathcal{S}(\theta + 1) = 1 + \mathcal{L}_\mathcal{S}(\theta)$.

Remark 2.3. Due to the R-reversibility of the map $\mathbf{G}$, the lift $\mathcal{L}_\mathcal{S}$ satisfies the equality $3/4 - \mathcal{L}_\mathcal{S}(\theta) = \mathcal{L}_\mathcal{S}^{-1}(3/4 - \theta)$. Also, we remark that the map $\mathcal{S}$ is increasing with respect to the variable θ and decreasing with respect to both parameters T_R and T_L.

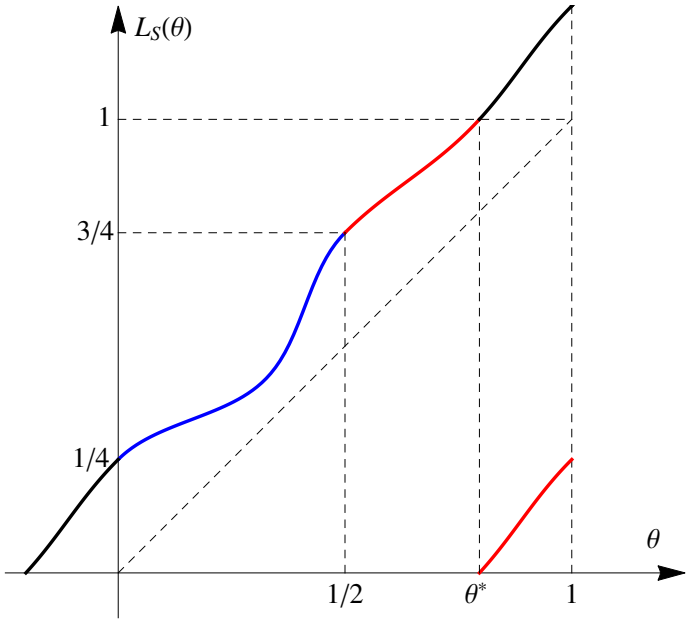

FIGURE 1. The graph of the map $\mathcal{S}$ in the square $[0,1]\times[0,1]$ and its natural lift $\mathcal{L}_\mathcal{S}$ in a case without fixed points when $T_L = 0.3$ and $T_R = 1$. The graph under the right (left) piece of the map $\mathcal{S}$ appears in blue (red). The graph of the extension associated to the lift $\mathcal{L}_\mathcal{S}$ appears in black. Note that for every pair of values T_R, T_L, there exists θ^* with $1/2 < \theta^* < 1$ such that $\mathcal{L}_\mathcal{S}(\theta^*) = 1$ and we have $\mathcal{L}_\mathcal{S}(0) = 1/4$, $\mathcal{L}_\mathcal{S}(1/2) = 3/4$.

We show in Figure 1 the graphs of the map $\mathcal{S}$ and its natural lift $\mathcal{L}_\mathcal{S}$ in a generic case without fixed points.

Our main results will concern the rotation number of the map $\mathcal{S}$ as the most useful magnitude in the study of its dynamics. We recall that the rotation number ρ is defined by

$$\rho = \lim_{k\to\infty} \frac{\mathcal{L}_\mathcal{S}^{(k)}(\theta) - \theta}{k} = \lim_{k\to\infty} \frac{\mathcal{L}_\mathcal{S}^{(k)}(\theta)}{k},$$

where $\mathcal{L}_\mathcal{S}^{(k)}$ stands for the k-iterate of the lift. It is well known that the rotation number of a preserving orientation homeomorphism on the circle can be computed by means of any lift and by using any initial value θ. Moreover, the rotation number is invariant under conjugation. Also, if the rotation number is rational, let us say $\rho = m/n$ with m

and n coprime, then the map $\mathcal{S}$ has a period-n orbit at least, and all the existing periodic orbits are period-n orbits. The dynamics of the map $\mathcal{S}$ in case of rational rotation number is characterized in [10] as follows.

Theorem 2.4. *If the rotation number ρ of the map $\mathcal{S}$ is rational, then the map $\mathcal{S}$ has at least a periodic orbit and one of the following three possibilities occurs.*

(a) *The map $\mathcal{S}$ has more than two periodic orbits. Then the map $\mathbf{G}$ is of finite order, i.e. $\mathbf{G}^{(n)} = I$ for some $n \geqslant 1$, and all its orbits are periodic.*
(b) *The map $\mathcal{S}$ has two periodic orbits. Then the map $\mathbf{G}$ has no periodic orbits. All the orbits of $\mathbf{G}$ diverge in modulus to $+\infty$ as the number of iterations $n \to \pm\infty$ with the exception of orbits lying over the rays corresponding to the two periodic orbits of $\mathcal{S}$. These exceptional orbits have modulus diverging to $+\infty$ in one time direction and converging to 0 in the other direction, with forward divergence for one, and backward divergence for the other.*
(c) *The map $\mathcal{S}$ has exactly one periodic orbit. Then the map $\mathbf{G}$ has exactly one periodic orbit (up to scaling) and all other orbits diverge in modulus to $+\infty$ as $n \to \pm\infty$.*

The computation of the rotation number is typically a very difficult task. Nevertheless, the rotation number of the map $\mathcal{S}$ in (10) was computed for some specific situations in [10]. We reproduce in next proposition the results of the quoted paper in a more compact form, giving also a clearer proof, to appear in Section 5. To simplify the writing, we introduce for any natural number n the values,

$$T_n = 2\cos\left(\frac{\pi}{n}\right) = 2\cos\omega_{2n}, \quad \text{where} \quad \omega_n = \frac{2\pi}{n}, \tag{13}$$

Proposition 2.5. *For the natural numbers $p, q \geqslant 2$, the following statements hold regarding the rotation number ρ of the map $\mathcal{S}$.*

(a) *If either $T_L \geqslant 2$ or $T_R \geqslant 2$, then $\rho = 0$.*
(b) *If $T_L < 0$, $T_R < 0$ and $T_L T_R \geqslant 4$, then $\rho = 1/2$.*
(c) *If $T_L = T_q$ and $|T_R| < 2$, so that we can write $T_R = 2\cos(2\pi\alpha)$ with $0 < \alpha < 1/2$, then*

$$\rho = \frac{2\alpha}{1 + 2\alpha q}.$$

If additionally, $T_R = T_p$, *that is* $2\alpha = 1/p$, *then* $\mathbf{G}^{(p+q)} = I$, *and*

$$\rho = \frac{1}{p+q}.$$

(d) *If* $T_L < 0, T_R < 0$ *and* $T_L T_R = 4\cos^2 \omega_{4n}$, *then* $\mathbf{G}^{(4n)} = I$ *and*

$$\rho = \frac{2n-1}{4n}.$$

From Proposition 2.1 (a) we easily get the following dual result of Proposition 2.5 (c) : if $T_R = T_p$, and $T_L = 2\cos(2\pi\alpha)$ with $0 < \alpha < 1/2$, then

$$\rho = \frac{2\alpha}{1+2\alpha p}.$$

Statement (c) in Proposition 2.5 along with its dual result allow us to draw a non-uniform grid in the parameter plane (T_R, T_L) constituted by two families of straight lines where the rotation number is known. One of these families starts at the line $T_R = 0$ and accumulates at the line $T_R = 2$, while the other one starts at $T_L = 0$ and accumulates at $T_L = 2$, see the blue lines in Figure 2. Also, in Figure 2 there appears the family of hyperbolas predicted by statement (d), where the rotation number is known too. This family starts at the hyperbola $T_R T_L = 2$ $(n = 2, \rho = 3/8)$ and accumulates at the hyperbola $T_R T_L = 4$ $(\rho = 1/2)$ as $n \to \infty$, see the red hyperbola in Figure 2.

The rest of the paper is organized as follows. In Section 3, regarding Figure 2, we obtain more information on the rotation number for map $\mathcal{S}$. In particular, we accurately describe some resonance tongues where the rotation number is constant. These results are summarize in Section 4 and some of their proofs appear in Section 5. Finally, we include one appendix, where the generalized Fibonacci polynomials are used to compute the powers of matrices.

3. Main Results

In this section we introduce our main results by considering the dynamical properties of the maps $\mathbf{G}$ and $\mathcal{S}$. From Proposition 2.5, we see that the transition of one of the traces through the critical value $T = 2$ leads to a dramatic change in the dynamical behavior, passing from a situation where the existence of periodic orbits is possible ($T_R < 2$ and $T_L < 2$) to a situation where $\rho = 0$ ($T_R \geqslant 2$ or $T_L \geqslant 2$).

First, we will look for period-two orbits of the map $\mathcal{S}$. It is easy to see that such periodic behavior must involve the two zones. By using as reference the branch $T_R, T_L < 0$ of the hyperbola $T_R T_L = 4$, we

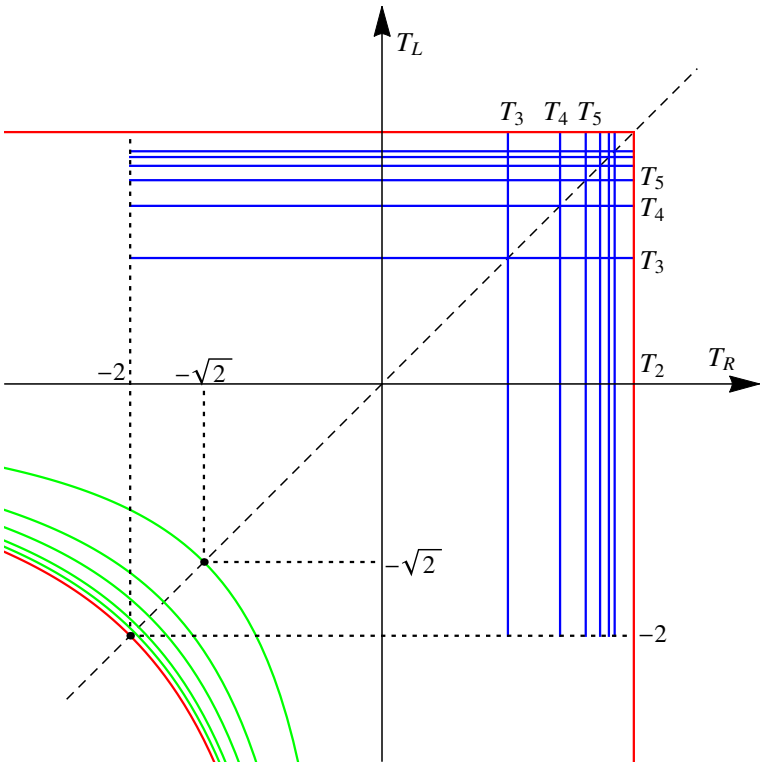

FIGURE 2. Lines where the rotation number is determined in Proposition 2.5. Note the symmetry with respect to the diagonal $T_R = T_L$. The red lines are predicted by statements (a) and (b). On the hyperbolas the rotation number is constant and on the straight blue lines the rotation number is strictly monotone.

establish some results about the existence of period-two orbits. Their proofs appear in Section 5.

Proposition 3.1. *Assume that $T_L < 2$ and $T_R < 2$ in map* **G**, *then the following statements hold for the map $\mathcal{S}$.*

(a) *If $T_R T_L < 4$, then the map $\mathcal{S}$ has no period-two orbits.*
(b) *If $T_R T_L = 4$, then the map $\mathcal{S}$ has only one period-two orbit.*
(c) *If $T_R T_L > 4$, then the map $\mathcal{S}$ has exactly two period-two orbits having opposite stabilities.*

Next, we study the cases, $T_R < 2$ and $T_L < 2$ with $T_R T_L < 4$, where periodic orbits with period greater than 2 are possible. Recall that the values T_n defined in (13) allow us to draw a non-uniform grid in the square $[-2, 2] \times [-2, 2]$ on the parameter plane (T_R, T_L), see Figure 2. In

the following and for the sake of brevity, we will denote the intersection point of the lines $T_R = T_p$ and $T_L = T_q$ in the parametric plane as

$$P_{p,q} = (T_p, T_q).$$

From statement (c) of Proposition 2.5, we have that the rotation number of map $\mathcal{S}$ at the point $P_{p,q}$ is $\rho = 1/(p+q)$. We will show that the points $P_{p,q}$ with $p, q \geqslant 2$ are shrinking points of some regions where our map has the same rotation number $\rho = 1/(p+q)$. Such regions are tongue-shaped or pocket-shaped with a 'sausage" structure and they are limited by two curves corresponding with saddle-node bifurcations of periodic orbits. Such curves intersect at the so-called shrinking points $P_{p,q}$.

The dynamical behavior of the map $\mathbf{G}$ at the shrinking points $P_{p,q}$ is determined in the next proposition whose proof appears in Section 5.

Proposition 3.2. *If $T_R = T_p$ and $T_L = T_q$ in map $\mathbf{G}$ with $p, q \geqslant 2$, then every point of the plane is period-$(p+q)$, that is $\mathbf{G}^{(p+q)} = I$. Furthermore, if $\mathbf{x} = (x, y)$ with $x \geqslant 0$ and $y < 0$, then $\mathbf{G}^{(p)}(\mathbf{x}) = A(T_p)^p \mathbf{x} = -\mathbf{x}$, and $\mathbf{G}^{(q)}(-\mathbf{x}) = A(T_q)^q(-\mathbf{x}) = \mathbf{x}$, and so*

$$\mathbf{G}^{(p+q)}(\mathbf{x}) = A(T_q)^q A(T_p)^p(\mathbf{x}) = \mathbf{x}.$$

Thus, when $T_R = T_p$ and $T_L = T_q$ the matrix $A(T_q)^q A(T_p)^p$ represents the map $\mathbf{G}^{(p+q)}$ for points with $x \geqslant 0, y < 0$ and the matrix $A(T_p)^p A(T_q)^q$ represents the map $\mathbf{G}^{(p+q)}$ for points with $x \leqslant 0, y > 0$. For points that do not meet such requirements, it can be shown that the map $\mathbf{G}^{(p+q)}$ is represented by a circular shift of the above matrix products.

To study the existence of periodic orbits of map $\mathcal{S}$ we need to consider powers of matrices $A(T)$. Firstly, according to Proposition A.2 (a) in Appendix A we have

$$A(T)^n = \begin{pmatrix} T & -1 \\ 1 & 0 \end{pmatrix}^n = \begin{pmatrix} \Psi_{n+1}(T) & -\Psi_n(T) \\ \Psi_n(T) & -\Psi_{n-1}(T) \end{pmatrix}, \tag{14}$$

where the functions Ψ_n, which are defined by the recurrence

$$\Psi_{n+1}(T) = T\Psi_n(T) - \Psi_{n-1}(T), \text{ with } \Psi_0(T) = 0, \Psi_1(T) = 1,$$

are a particular instance of generalized Fibonacci polynomials, see Appendix A. From (14) it follows for any natural numbers r, s that

$$A(T_L)^r A(T_R)^s = \begin{pmatrix} \Psi^-_{r+1}\Psi^+_{s+1} - \Psi^-_r\Psi^+_s & \Psi^-_r\Psi^+_{s-1} - \Psi^-_{r+1}\Psi^+_s \\ \Psi^-_r\Psi^+_{s+1} - \Psi^-_{r-1}\Psi^+_s & \Psi^-_{r-1}\Psi^+_{s-1} - \Psi^-_r\Psi^+_s \end{pmatrix} \tag{15}$$

where in order to simplify notation we have written Ψ_n^+, Ψ_n^- instead of $\Psi_n(T_R)$ and $\Psi_n(T_L)$, respectively. Also, the notation $(\cdot)_{12}$ stands for the top right entry of the matrix between parentheses.

3.1. **Periodic orbits of map $\mathcal{S}$ with a point at the boundary manifold Σ..** We first consider the special periodic orbits having a point at the boundary manifold by using the notation,

$$\mathbf{u}_0 = (0, -1), \quad \mathbf{u}_1 = (1, 0).$$

Definition 3.3. A periodic orbit of map $\mathcal{S}$ containing either the point $\mathbf{u}_0$ or the point $-\mathbf{u}_0$, is termed a periodic $\mathcal{B}$-orbit.

Clearly, the map $\mathcal{S}$ can have none, one or two periodic $\mathcal{B}$-orbits. It is worth noting that a periodic $\mathcal{B}$-orbit containing the point $\mathbf{u}_0$, also contains the point $\mathbf{u}_1$ because $\mathbf{G}(\mathbf{u}_0) = \mathbf{u}_1$ for every value of parameters. If there exists a periodic $\mathcal{B}$-orbit containing the point $\mathbf{u}_0$, then by the reversibility of Proposition 2.1 another periodic $\mathcal{B}$-orbit, not necessarily different, containing the points $-\mathbf{u}_0$ and $-\mathbf{u}_1$ also exists. If there exists only one periodic $\mathcal{B}$-orbit, it must contain the four points $\pm\mathbf{u}_0, \pm\mathbf{u}_1$ and in such a case the periodic $\mathcal{B}$-orbit will be called periodic $\mathcal{B}^0$-orbit.

Note that when we are at $P_{p,q}$ with $p, q \geqslant 2$, from Proposition 3.2 and having in mind the continuity of the map we get

$$\mathbf{G}^{(p+q)}(\mathbf{u}_0) = A(T_q)^q A(T_p)^p \mathbf{u}_0 = A(T_q)^{q-1} A(T_p)^{p+1} \mathbf{u}_0,$$

and so the map $\mathcal{S}$ has one periodic $\mathcal{B}^0$-orbit. Hence the two matrices $A(T_q)^q A(T_p)^p$, and $A(T_q)^{q-1} A(T_p)^{p+1}$ are admissible for the point $\mathbf{u}_0$ while the matrices $A(T_p)^p A(T_q)^q$, and $A(T_p)^{p-1} A(T_q)^{q+1}$ are admissible for the point $-\mathbf{u}_0$. In the sequel, we will use the existence of periodic $\mathcal{B}^0$-orbits at the point $P_{p,q}$, as the unperturbed situation in looking for other periodic orbits.

Regarding the periodic $\mathcal{B}$-orbits our first result is the following.

Proposition 3.4. *If $p \geqslant q \geqslant 2$, $T_p < T_R < T_{p+1}$ and $T_{q-1} < T_L < T_q$, then the following two equalities hold*

$$\begin{aligned} \mathbf{G}^{(p+q)}(\mathbf{u}_0) &= A(T_L)^{q-1} A(T_R)^{p+1} \mathbf{u}_0, \\ \mathbf{G}^{(p+q)}(-\mathbf{u}_0) &= A(T_R)^p A(T_L)^q (-\mathbf{u}_0), \end{aligned} \tag{16}$$

and the map $\mathcal{S}$ has two periodic $\mathcal{B}$-orbits when

$$\left(A(T_L)^{q-1} A(T_R)^{p+1}\right)_{12} = \left(A(T_R)^p A(T_L)^q\right)_{12} = \Psi_{q-1}^- \Psi_p^+ - \Psi_q^- \Psi_{p+1}^+ = 0. \tag{17}$$

Proof. From Lemma 5.2 in Section 5.3 we directly obtain (16), showing the admisibility of the involved products of matrices. The map $\mathcal{S}$ has a periodic $\mathcal{B}$-orbit when either

$$A(T_L)^{q-1}A(T_R)^{p+1}\mathbf{u}_0 = \lambda\mathbf{u}_0 \quad \text{or} \quad A(T_R)^p A(T_L)^q(-\mathbf{u}_0) = -\mu\mathbf{u}_0$$

for some $\lambda, \mu \in \mathbb{R}^+$. Equivalently, we need that equality (17) be satisfied, see (15). Under our hypotheses, $\mathbf{u}_0$ is neither an eigenvector of matrices $A(T_R)^{p+1}$ nor $A(T_L)^q$, see Proposition A.2 (a) and 42. Thus, this periodic $\mathcal{B}$-orbit cannot be a $\mathcal{B}^0$-orbit and then by reversibility another periodic $\mathcal{B}$-orbit exists and the proof is done. □

Next, for $p \geqslant 1$ and $q \geqslant 2$, having in mind (17) we introduce the function

$$\mathcal{F}_{p,q}(T_R, T_L) = \Psi_p(T_R)\Psi_{q-1}(T_L) - \Psi_{p+1}(T_R)\Psi_q(T_L). \tag{18}$$

We will see that the equation $\mathcal{F}_{p,q}(T_R, T_L) = 0$ allows us to define a function $T_L = \mathcal{T}^{\mathrm{B}}_{p,q}(T_R)$ satisfying $\mathcal{F}_{p,q}(T_R, \mathcal{T}^{\mathrm{B}}_{p,q}(T_R)) = 0$ such that the map $\mathcal{S}$ has two periodic $\mathcal{B}$-orbits on its graph.

Remark 3.5. From (18) and the equality $\mathcal{F}_{p,q}(T_R, \mathcal{T}^{\mathrm{B}}_{p,q}(T_R)) = 0$ we obtain $\mathcal{F}_{q-1,p+1}(\mathcal{T}^{\mathrm{B}}_{p,q}(T_L), T_L) = 0$. Taking into account the function $\mathcal{T}^{\mathrm{B}}_{q-1,p+1}$, we have

$$\mathcal{F}_{q-1,p+1}(T_R, \mathcal{T}^{\mathrm{B}}_{q-1,p+1}(T_R)) = 0,$$

and so we get $\mathcal{T}^{\mathrm{B}}_{p,q} = (\mathcal{T}^{\mathrm{B}}_{q-1,p+1})^{-1}$.

For low values of the parameters p or q we can explicitly obtain the function $\mathcal{T}^{\mathrm{B}}_{p,2}$, while for greater values of p and q we resort to the Intermediate Value and Implicit Function theorems to study the functions $\mathcal{T}^{\mathrm{B}}_{p,q}$. We postpone the proof of the following proposition to Section 5.

Proposition 3.6. *For all natural numbers $p \geqslant 1$ and $q \geqslant 2$ there exists one function $T_L = \mathcal{T}^{B}_{p,q}(T_R)$ satisfying $\mathcal{F}_{p,q}(T_R, \mathcal{T}^{B}_{p,q}(T_R)) = 0$, such that the map $\mathcal{S}$ has two periodic $\mathcal{B}$-orbits at the non-shrinking points (T_R, T_L) on its graph and the following statements hold.*

(a) *If $q = 2$ and $p = 1$, then $\mathcal{T}^{B}_{1,2}(T_R) = 1/T_R$, defined for $T_R < 0$.*
(b) *If $q = 2$ and $p \geqslant 2$ we have*

$$\mathcal{T}^{B}_{p,2}(T_R) = \frac{\Psi_p(T_R)}{\Psi_{p+1}(T_R)},$$

which is defined for $T_p \leqslant T_R < T_{p+1}$ and satisfies the relations,

$$\mathcal{T}^{B}_{p,2}(T_R) < T_2 = 0, \quad \mathcal{T}^{B}_{p,2}(T_p) = T_2, \quad \frac{d\mathcal{T}^{B}_{p,2}}{dT_R}(T_p) = -\frac{p(T_2^2 - 4)}{2(T_p^2 - 4)}.$$

(c) *If* $q \geqslant 3$ *and* $p = 1$, *then* $\mathcal{T}^B_{1,q}(T_R) = (\mathcal{T}^B_{q-1,2})^{-1}(T_R)$, *which is defined for* $T_R < 0$ *and satisfies*

$$\mathcal{T}^B_{1,q}(T_2) = T_{q-1} \leqslant \mathcal{T}^B_{1,q}(T_R) < T_q.$$

(d) *If* $q \geqslant 3$ *and* $p \geqslant 2$ *then* $\mathcal{T}^B_{p,q}(T_R)$ *is defined for* $T_p \leqslant T_R \leqslant T_{p+1}$ *with*

$$\mathcal{T}^B_{p,q}(T_p) = T_q, \quad \mathcal{T}^B_{p,q}(T_{p+1}) = T_{q-1}, \quad T_{q-1} \leqslant \mathcal{T}^B_{p,q}(T_R) \leqslant T_q.$$

The derivatives of the function $\mathcal{T}^B_{p,q}$ *at the points* $P_{p,q}$, $P_{p+1,q-1}$ *are*

$$\frac{d\mathcal{T}^B_{p,q}}{dT_R}(P_{p,q}) = -\frac{p(T_q^2-4)}{q(T_p^2-4)}, \quad \frac{d\mathcal{T}^B_{p,q}}{dT_R}(P_{p+1,q-1}) = -\frac{(p+1)(T_{q-1}^2-4)}{(q-1)(T_{p+1}^2-4)}.$$

Note that from statements (b) and (c) in Proposition 3.6 we deduce that at the parameter points

$$(T_R, T_L) = \left(\frac{\Psi_{q-1}(T_L)}{\Psi_q(T_L)}, T_L\right) \text{ with } T_L < 0,$$

the map $\mathcal{S}$ has two periodic $\mathcal{B}$-orbits.

In the following Remark we describe the dynamical behavior of the map $\mathcal{S}$ at parametric points close enough to the graph of $\mathcal{T}^B_{p,q}$.

Remark 3.7. Let P_A be a point belonging to the rectangle $[T_p, T_{p+1}] \times [T_{q-1}, T_q]$ in the parameter plane and close enough to the graph of the function $\mathcal{T}^B_{p,q}$. At the point P_A the two periodic $\mathcal{B}$-orbits existing on the graph of the function $\mathcal{T}^{\mathrm{B}}_{p,q}$ become a couple of standard periodic orbits. This couple of periodic orbits can be considered as the result of a perturbation of the two periodic $\mathcal{B}$-orbits. If P_A is located below the graph of the function $\mathcal{T}^B_{p,q}$, the couple of periodic orbits is determined by the matrix $A(T_L)^q A(T_R)^p$ because the perturbation makes the point of the periodic $\mathcal{B}$-orbit on the boundary line Σ to enter Σ^-. However, if P_A is located above the graph of the function $\mathcal{T}^B_{p,q}$, the two periodic orbits are determined by the matrix $A(T_L)^{q-1}A(T_R)^{p+1}$ because the point of the two periodic $\mathcal{B}$-orbit located on the boundary line Σ enters Σ^+ after the perturbation.

Next, we will see that the couple of periodic orbits exists until the parameter point (T_R, T_L) reaches the graph of a certain function, to be defined below, where both periodic orbits disappear in a saddle node bifurcation.

3.2. **Saddle-node bifurcation of periodic orbits.** Our next results concern the trace of the matrix $A(T_L)^q A(T_R)^p$. If we denote $\mathbb{T}_{p,q}(T_R, T_L) = \text{trace}(A(T_L)^q A(T_R)^p)$, then from (15) we have

$$\mathbb{T}_{p,q}(T_R, T_L) = \Psi^+_{p+1}\Psi^-_{q+1} - 2\Psi^+_p\Psi^-_q + \Psi^+_{p-1}\Psi^-_{q-1}. \tag{19}$$

Assume that the matrix $A(T_L)^q A(T_R)^p$ represents the map $\mathbf{G}^{(p+q)}$ for an appropriate initial point. If $\mathbb{T}_{p,q}(T_R, T_L) = 2$, there exists a double eigenvalue, so that the map $\mathbf{G}^{(p+q)}$ has just one invariant ray, and so the map $\mathcal{S}$ has only one periodic orbit on its graph. Regarding Proposition 3.1, this situation is a boundary condition between the existence or non existence of periodic orbits with period $p+q$. In the sequel, we will see that the equation $\mathbb{T}_{p,q}(T_R, T_L) = 2$ allows us to define a function $T_L = \mathcal{T}_{p,q}(T_R)$ satisfying $\mathbb{T}_{p,q}(T_R, \mathcal{T}_{p,q}(T_R)) = 2$ such that the map $\mathcal{S}$ has only one periodic orbit.

Remark 3.8. From (19) and the equality $\mathbb{T}_{p,q}(T_R, \mathcal{T}_{p,q}(T_R)) = 2$ we obtain $\mathbb{T}_{q,p}(\mathcal{T}_{p,q}(T_L), T_L) = 2$. Since the function $\mathcal{T}_{q,p}$ satisfies

$$\mathbb{T}_{q,p}(T_R, \mathcal{T}_{q,p}(T_R)) = 0,$$

we get $\mathcal{T}_{p,q} = (\mathcal{T}_{q,p})^{-1}$.

For low values of the parameters p or q we can explicitly obtain the function $\mathcal{T}_{p,q}$, while for greater values of p and q we resort to the Intermediate Value and Implicit Function theorems to study the functions $\mathcal{T}_{p,q}$. The proof of the next result appears in Section 5.

Proposition 3.9. *For all natural numbers $p \geqslant q$ there exists one function $T_L = \mathcal{T}_{p,q}(T_R)$ satisfying $\mathcal{T}_{p,q}(T_p) = T_q$ and $\mathbb{T}_{p,q}(T_R, \mathcal{T}_{p,q}(T_R)) = 2$ such that the map $\mathcal{S}$ has only one periodic orbit at the non-shrinking points (T_R, T_L) on its graph and the following statements hold.*

(a) *If $p \geqslant q \geqslant 3$, then $\mathcal{T}_{p,q}$ is defined for $T_{p-1} \leqslant T_R \leqslant T_{p+1}$ with*

$$T_{q-1} = \mathcal{T}_{p,q}(T_{p+1}) \leqslant \mathcal{T}_{p,q}(T_R) \leqslant \mathcal{T}_{p,q}(T_{p-1}) = T_{q+1}.$$

The first order local expansions of the function $\mathcal{T}_{p,q}$ at the points $T_R = T_{p-1}, T_R = T_p$ and $T_R = T_{p+1}$ are

$$T_L = \mathcal{T}_{p,q}(T_R) = T_{q+1} - \frac{(p-1)(T^2_{q+1}-4)}{(q+1)(T^2_{p-1}-4)}(T_R - T_{p-1}) + \cdots \tag{20}$$

$$T_L = \mathcal{T}_{p,q}(T_R) = T_q - \frac{p(T_q-2)}{q(T_p-2)}(T_R - T_p) + \cdots \tag{21}$$

$$T_L = \mathcal{T}_{p,q}(T_R) = T_{q-1} - \frac{(p+1)(T^2_{q-1}-4)}{(q-1)(T^2_{p+1}-4)}(T_R - T_{p+1}) + \cdots \tag{22}$$

(b) *If $p \geqslant q = 2$ then the function $\mathcal{T}_{p,q}$ reduces to*

$$\mathcal{T}_{p,2}(T_R) = \frac{\Psi_{p+1}(T_R) + \Psi_p(T_R) + 1}{\Psi_{p+1}(T_R)} \tag{23}$$

which is defined for $T_{p-1} \leqslant T_R < T_{p+1}$ and satisfies

$$-\infty < \mathcal{T}_{p,2}(T_R) \leqslant \mathcal{T}_{p,2}(T_{p-1}) = T_3 = 1.$$

(c) *If $q = 1$ and $p \geqslant 3$ then the function $\mathcal{T}_{p,q}$ reduces to*

$$\mathcal{T}_{p,1}(T_R) = 2\frac{1 + \Psi_p(T_R)}{\Psi_{p+1}(T_R)}$$

which is defined for $T_{p-1} \leqslant T_R < T_{p+1}$ and satisfies

$$-\infty < \mathcal{T}_{p,1}(T_R) \leqslant \mathcal{T}_{p,1}(T_{p-1}) = T_2 = 0.$$

(d) *If $q = 1$ and $p = 2$ then the function $\mathcal{T}_{p,q}(T_R)$ reduces to*

$$\mathcal{T}_{2,1}(T_R) = \frac{2}{T_R - 1},$$

which is defined for $T_R < T_3 = 1$ and satisfies

$$-\infty < \mathcal{T}_{2,1}(T_R) < T_2 = 0.$$

Some members of the family $\mathcal{T}_{p,1}(T_R)$ are,

$$\mathcal{T}_{1,1} = \frac{4}{T_R}, \quad \mathcal{T}_{2,1} = \frac{2}{T_R - 1}, \quad \mathcal{T}_{3,1} = \frac{2T_R}{T_R^2 - 2}, \quad \mathcal{T}_{4,1} = \frac{2(T_R - 1)}{T_R^2 - T_R - 1}$$

$$\mathcal{T}_{5,1} = \frac{2(T_R^2 - 2)}{T_R(T_R^2 - 3)}, \quad \mathcal{T}_{6,1} = \frac{2(T_R^2 - T_R - 1)}{T_R^3 - R_R^2 - 2T_R + 1}, \quad \mathcal{T}_{7,1} = \frac{2(T_R^3 - 3T_R)}{T_R^4 - 4T_R^2 + 2} \cdots$$

while for the family $\mathcal{T}_{p,2}(T_R)$ we have

$$\mathcal{T}_{2,2} = \frac{T_R}{T_R - 1}, \quad \mathcal{T}_{3,2} = \frac{T_R^2 + T_R - 2}{T_R^2 - 2}, \quad \mathcal{T}_{4,2} = \frac{T_R^2 - 2}{T_R^2 - T_R - 1},$$

$$\mathcal{T}_{5,2} = \frac{T_R^3 + T_R^2 - 3T_R - 2}{T_R^3 - 3T_R}, \quad \mathcal{T}_{6,2} = \frac{T_R^3 - 3T_R}{T_R^3 - T_R^2 - 2T_R + 1}, \ldots$$

In the next remark we state some results obtained when we apply Proposition 3.9 at the points $P_{p+1,q-1}$ and $P_{p-1,q+1}$ for $q \geqslant 3$.

Remark 3.10. From Proposition 3.9 there exists one function $T_L = \mathcal{T}_{p-1,q+1}(T_R)$ with $T_{q+1} = \mathcal{T}_{p-1,q+1}(T_{p-1})$ defined for $T_{p-2} \leqslant T_R \leqslant T_p$ and satisfying

$$T_q = \mathcal{T}_{p-1,q+1}(T_p) \leqslant \mathcal{T}_{p-1,q+1}(T_R) \leqslant \mathcal{T}_{p-1,q+1}(T_{p-2}) = T_{q+2}.$$

Also, there exists one function $T_L = \mathcal{T}_{p+1,q-1}(T_R)$ with $T_{q-1} = \mathcal{T}_{p+1,q-1}(T_{p+1})$ defined for $T_p \leqslant T_R \leqslant T_{p+2}$ and satisfying

$$T_{q-2} = \mathcal{T}_{p+1,q-1}(T_{p+2}) \leqslant \mathcal{T}_{p+1,q-1}(T_R) \leqslant \mathcal{T}_{p+1,q-1}(T_p) = T_q,$$

such that at the non-shrinking points on the graphs of the two functions $\mathcal{T}_{p-1,q+1}$ and $\mathcal{T}_{p+1,q-1}$, the map S has only one periodic orbit. Moreover, the two functions $\mathcal{T}_{p-1,q+1}$ and $\mathcal{T}_{p+1,q-1}$ have the same local expansion at the point $P_{p,q}$ namely,

$$T_L = T_q - \frac{p(T_q^2-4)}{q(T_p^2-4)}(T_R - T_p) + \cdots$$

Now, we are in position of establishing the dynamical behavior of our system in a neighborhood of the point $P_{p,q}$. Since Proposition 2.1 enforces the symmetry of the different graphs with respect to the diagonal $T_R = T_L$, we only describe the cases $p \geqslant q$.

From propositions 3.6, 3.9 and Remark 3.10, the graph of the five functions $\mathcal{T}^B_{p,q}$, $\mathcal{T}^B_{p-1,q+1}$, $\mathcal{T}_{p,q}$, $\mathcal{T}_{p-1,q+1}$ and $\mathcal{T}_{p+1,q-1}$ meet at the point $P_{p,q}$ satisfying the equalities,

$$\frac{d\mathcal{T}^B_{p-1,q+1}}{dT_R} = \frac{d\mathcal{T}^B_{p,q}}{dT_R} = \frac{d\mathcal{T}_{p-1,q+1}}{dT_R} = \frac{d\mathcal{T}_{p+1,q-1}}{dT_R} = -\frac{p(T_q^2-4)}{q(T_p^2-4)} < 0.$$

Also, for $p \geqslant q$ we have the inequality,

$$\frac{d\mathcal{T}_{p,q}}{dT_R} = -\frac{p(T_q-2)}{q(T_p-2)} \leqslant -\frac{p(T_q^2-4)}{q(T_p^2-4)} < 0.$$

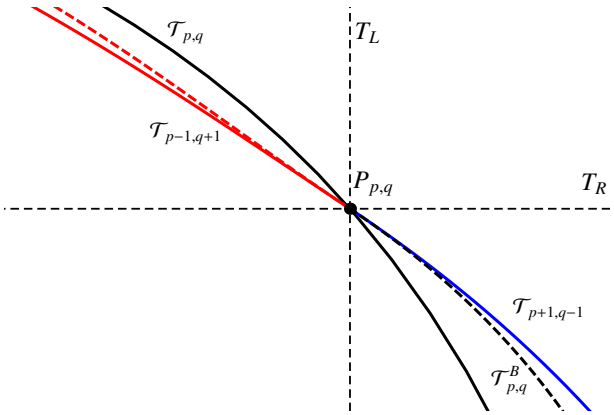

FIGURE 3. Significant lines around the point $P_{p,q}$ with $p > q$. The graphs of the functions $\mathcal{T}_{p,q}$,$\mathcal{T}_{p+1,q-1}$ and $\mathcal{T}_{p-1,q+1}$ which appear in black, blue and red respectively, and the graphs of the functions $\mathcal{T}^B_{p,q}$ and $\mathcal{T}^B_{p-1,q+1}$ (not labelled) which appear dashed in black and red respectively are tangent at the point $P_{p,q}$.

When $p > q$, the graphs of the above five functions appear in Figure 3. In the quoted figure we distinguish the following four sectors:

(a) The sector determined by the graphs of $\mathcal{T}_{p,q}$ and $\mathcal{T}^B_{p,q}$ and the sector determined by $\mathcal{T}_{p,q}$ and $\mathcal{T}^B_{p-1,q+1}$ where the matrix product $A(T_L)^q A(T_R)^p$ is admissible.
(b) The sector determined by the graphs of $\mathcal{T}^B_{p,q}$ and $\mathcal{T}_{p+1,q-1}$ where the matrix product $A(T_L)^{q-1} A(T_R)^{p+1}$ is admissible.
(c) The sector determined by the graphs of $\mathcal{T}^B_{p-1,q+1}$ and $\mathcal{T}_{p-1,q+1}$ where the matrix product $A(T_L)^{q+1} A(T_R)^{p-1}$ is admissible.

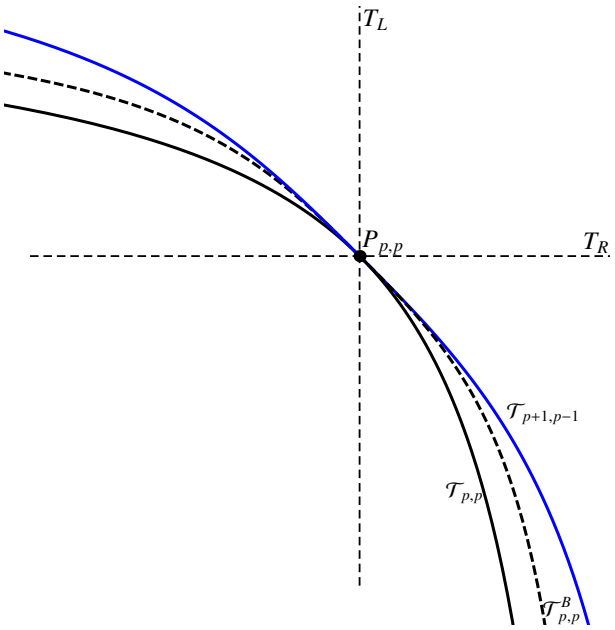

FIGURE 4. Significant lines for $T_R \geqslant T_L$ at the point $P_{p,p}$. The graph of the function $\mathcal{T}_{p+1,p-1}$ appears in blue, while the graph of the function $\mathcal{T}_{p,p}$ appears in black. The graph of the function $\mathcal{T}^B_{p,p}$ appears dashed in black. The graph of the above three functions at the point $P_{p,p}$ are tangent, being the commom derivative equal to -1. Those lines have their symmetrical counterpart with respect to the diagonal $T_R = T_L$.

When $p = q$ the graph of the above five functions meet at the point $P_{p,p}$ with a slope equal to -1, see Figure 4. In this figure we distinguish four sectors: the sector determined by the graphs of $\mathcal{T}_{p,p}$ and $\mathcal{T}^B_{p,p}$ where the matrix product $A(T_L)^p A(T_R)^p$ is admissible, the sector determined by the graphs of $\mathcal{T}^B_{p,p}$ and $\mathcal{T}_{p+1,p-1}$ where the matrix product $A(T_L)^{p-1} A(T_R)^{p+1}$ is admissible and its corresponding symmetrical sectors with respect to the line $T_R = T_L$.

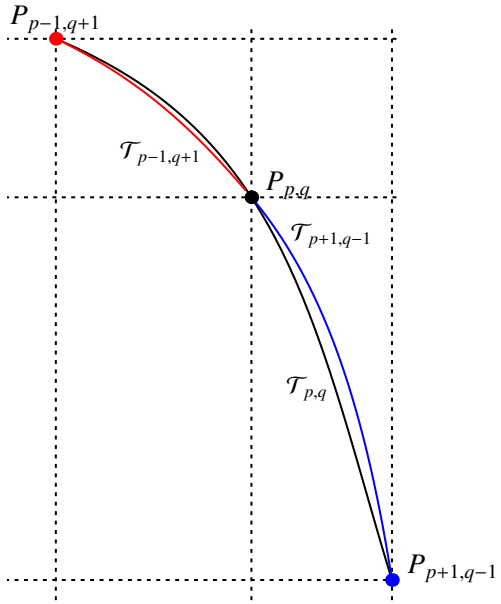

FIGURE 5. The graph of the functions $\mathcal{T}_{p-1,q+1}$ (in red), $\mathcal{T}_{p,q}$ (in black), and $\mathcal{T}_{p+1,q-1}$ (in blue), when the points $P_{p-1,q+1}$ and $P_{p-1,q+1}$ are below the line $T_R = T_L$.

3.3. **The structure of resonance regions.** The points $P_{p-1,q+1}$ and $P_{p,q}$ are linked by the graphs of the functions $\mathcal{T}_{p-1,q+1}$ and $\mathcal{T}_{p,q}$, while the points $P_{p,q}$ and $P_{p+1,q-1}$ are linked by the graphs of the functions $\mathcal{T}_{p,q}$ and $\mathcal{T}_{p+1,q-1}$. These three functions make up two lobes or beads on the interval $[T_{p-1}, T_{p+1}]$ enclosing a sausage-like or necklace-like region where the map $\mathcal{S}$ has two $p+q$ periodic orbits. In passing through the graphs of the functions $\mathcal{T}_{p-1,q+1}$, $\mathcal{T}_{p,q}$ and $\mathcal{T}_{p-1,q+1}$ the two periodic orbits disappear by means of a saddle node bifurcation.

We have three different scenarios depending on the relative position of the points $P_{p-1,q+1}$ and $P_{p,q}$ with respect to the line $T_R = T_L$.

The first scenario appears when both points $P_{p-1,q+1}$ and $P_{p,q}$ are below the line $T_R = T_L$. The sausage-like region corresponding to this case is sketched in Figure 5. Note that the graphs of the functions $\mathcal{T}_{p-1,q+1}$, and $\mathcal{T}_{p+1,q-1}$ continuously glue and they both transversally cut the graph of the function $\mathcal{T}_{p,q}$ at the point $P_{p,q}$.

The second scenario appears when $P_{p,q}$ is on the line $T_R = T_L$, that is when $p = q$. The sausage-like region corresponding to this case is sketched in the upper part of Figure 6. Note that the graphs of the functions $\mathcal{T}_{p-1,q+1}$, and $\mathcal{T}_{p+1,q-1}$ continuously glue at the point $P_{p,q}$, but

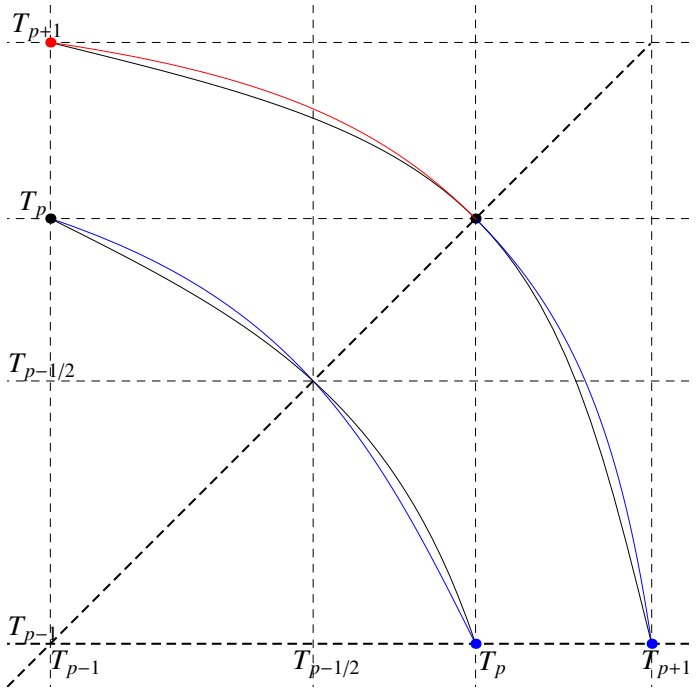

FIGURE 6. Crosses of the sausage-like structure through the diagonal. At the point $P_{p,p}$, the graphs of the functions $\mathcal{T}_{p-1,p+1}$ (in red), $\mathcal{T}_{p+1,p-1}$ (in blue) and $\mathcal{T}_{p,p}$ (in black), tangentially meet. At the point $(T_{p-1/2}, T_{p-1/2})$, the graphs of the function $\mathcal{T}_{p-1,p}$ (in black), transversally cuts the graph of the function $\mathcal{T}_{p,p-1}$ in blue. Note the symmetry with respect to the line $T_R = T_L$.

in contrast with the case of the first scenario, they both are tangent to the graph of the function $\mathcal{T}_{p,q}$ at the point $P_{p,q}$.

The last scenario appears when the points $P_{p-1,q+1}$ and $P_{p,q}$ are located at different sides of the line $T_R = T_L$, that is when $q = p-1$. We will see below that the graphs of the functions $\mathcal{T}^B_{p-1,p}$, and $\mathcal{T}_{p-1,p}$ and $\mathcal{T}_{p,p+1}$ cut the line at the point $\widehat{P}_p = (\widehat{T}_p, \widehat{T}_p)$ where $p \geqslant 2$ and

$$\widehat{T}_p = T_{p-\frac{1}{2}} = 2\cos\left(\frac{\pi}{p-\frac{1}{2}}\right) = 2\cos\omega_{2p-1}.$$

The next proposition is a direct consequence of Remark A.3 in the ppendix A.

Proposition 3.11. *When $T_R = T_L = \widehat{T}_p$, then every point is $2p-1$ periodic for the map $\mathbf{G}$ and the map $\mathcal{S}$ has two periodic $\mathcal{B}$-orbits.*

Since the period of the above two periodic orbits is odd, we remark that the quoted periodic orbits are not periodic $\mathcal{B}^0$-orbits. Next, the behavior of the functions $\mathcal{T}^{\mathrm{B}}_{p-1,p}$, $\mathcal{T}_{p-1,p}$ and $\mathcal{T}_{p,p+1}$, introduced in propositions 3.6 and 3.9, in a neighborhood of the point $\widehat{P}_p$, is given without proof.

Proposition 3.12. *For any integer $p \geqslant 2$, the following statements hold.*

(a) *The function $\mathcal{F}_{p-1,p}(T_R, T_L)$ defined in* (18) *satisfies $\mathcal{F}_{p-1,p}(\widehat{P}_p) = 0$, and the function $\mathcal{T}^{B}_{p-1,p}$ defined in Proposition 3.6 satisfies $\widehat{T}_p = \mathcal{T}^{B}_{p-1,p}(\widehat{T}_p)$ and its local expansion at the point $T_R = \widehat{T}_p$ is*

$$T_L = \mathcal{T}^{B}_{p-1,p}(T_R) = \widehat{T}_p - (T_R - \widehat{T}_p) + \cdots$$

(b) *The functions $\mathbb{T}_{p-1,p}(T_R, T_L)$ and $\mathbb{T}_{p,p-1}(T_R, T_L)$ defined in* (19) *satisfy $\mathbb{T}_{p-1,p}(\widehat{P}_p) = \mathbb{T}_{p,p-1}(\widehat{P}_p) = 2$, and the functions $\mathcal{T}_{p-1,p}$ and $\mathcal{T}_{p,p+1}$ defined in Proposition 3.9 satisfy*

$$\mathcal{T}_{p-1,p}(\widehat{T}_p) = \mathcal{T}_{p,p-1}(\widehat{T}_p) = \widehat{T}_p.$$

The expansions of the functions $\mathcal{T}_{p-1+k,p-k}$ for $k \in \{0, 1\}$ at the point $\widehat{T}_p$ are

$$T_L = \mathcal{T}_{p-1+k,p-k}(T_R) = \widehat{T}_p - \left(\frac{p - \Gamma_p}{p - 1 + \Gamma_p}\right)^{1-2k} (T_R - \widehat{T}_p) + \cdots$$

where $\Gamma_p = (2 + T_p)^{-1/2}$.

The sausage-like regions associated to the shrinking points $\widehat{P}_p = (T_{p-\frac{1}{2}}, T_{p-\frac{1}{2}})$ is sketched in the lower part of Figure 6, where we can see how the graphs of the functions $\mathcal{T}_{p-1,p}$ and $\mathcal{T}_{p,p+1}$ intersect at the point $\widehat{P}_p$, changing their relative position.

4. Conclusions

We have shown that the so-called normal form introduced in [14] and later studied by [3], among others, is in fact a canonical form for continuous 2D planar maps with two zones separated by a straight line.

We have restricted our attention to the homogeneous case, where the only fixed point is the origin. We have revisited some previous works [10]-[12] regarding area-preserving maps with the aim of giving analytical descriptions for the boundaries of some parameter regions where the maps have a constant rotation number. Such regions exhibit a very intricate sausage-like shape organized around certain shrinking points.

Thus, for each value $n \geqslant 3$, we have identified some resonance regions in the parametric plane (T_R, T_L) where the map $\mathcal{S}$ has two period-n orbits and its rotation number is $\rho = 1/n$. These resonance regions are symmetric with respect to the line $T_R = T_L$ and are determined by the graphs of the functions $\mathcal{T}_{p,q}$, which were introduced in Proposition 3.9.

When $n = 3$ and $n = 4$, the resonance region consists of only two sectors collapsing at the point $(T_R, T_L) = (-1, -1)$ for $n = 3$ and at the origin of the parameter plane for $n = 4$. These sectors are limited by the graphs of the functions $\mathcal{T}_{1,2}$ and $\mathcal{T}_{2,1}$ when $n = 3$ and by the graphs of the functions $\mathcal{T}_{1,3}, \mathcal{T}_{3,1}$ and $\mathcal{T}_{2,2}$ when $n = 4$, as indicated in Section 3.

When $n \geqslant 5$, the corresponding resonance regions make up a bead-like or sausage-like structure shrinking at the points

$$P_{n-k,k} = (T_{n-k}, T_k)\,, \quad T_n = 2\cos\left(\frac{\pi}{n}\right), \quad 2 \leqslant k \leqslant n-2.$$

Furthermore, when $n = 2p$, the sausage-like structure has $n-4$ bounded regions plus two unbounded terminal regions and crosses the diagonal $T_R = T_L$ through the point $P_{p,p}$ where the graphs of the functions $\mathcal{T}_{p-1,p+1}, \mathcal{T}_{p,p}$ and $\mathcal{T}_{p+1,p-1}$ are tangent, see Figure 7. When $n = 2p-1$, the sausage-like structure has $n-3$ bounded regions plus two unbounded terminal regions and crosses the line $T_R = T_L$ through the shrinking point $\widehat{P}_p = P_{p-\frac{1}{2},p-\frac{1}{2}}$, where the graphs of the functions $\mathcal{T}_{p-1,p}$ and $\mathcal{T}_{p,p-1}$ have inverse slopes. see again Figure 7.

In Figure 7, points $P_{p,q}$ and curves $\mathcal{T}_{p,q}$ are drawn in black, blue, red and green for $q = 1, 2, 3, 4$ respectively. Dashed lines are asociated to points $P_{p,q}$ with $q > p$. We realize that the resonance region enclosed by the graph of the functions $\mathcal{T}_{p,2}$ and $\mathcal{T}_{p+1,1}$ has no shrinking points for $T_L < T_2 = 0$, and so the points $P_{p,1}$ and their symmetrical points $P_{1,q}$ are not shrinking points.

We remark that a complete bifurcation set should include the possible resonance regions associated to rational rotation numbers $\rho = m/n$. In fact, these rotation numbers can be easily detected along the lines defined in Proposition 2.5(c). However, to determine the boundaries of these other resonance regions, one has to extend the techniques used to show Proposition 3.2, by adequately combining powers of both matrices. Even we have obtained partial results in such a direction, the required computations are rather cumbersome and are out of the scope of this work.

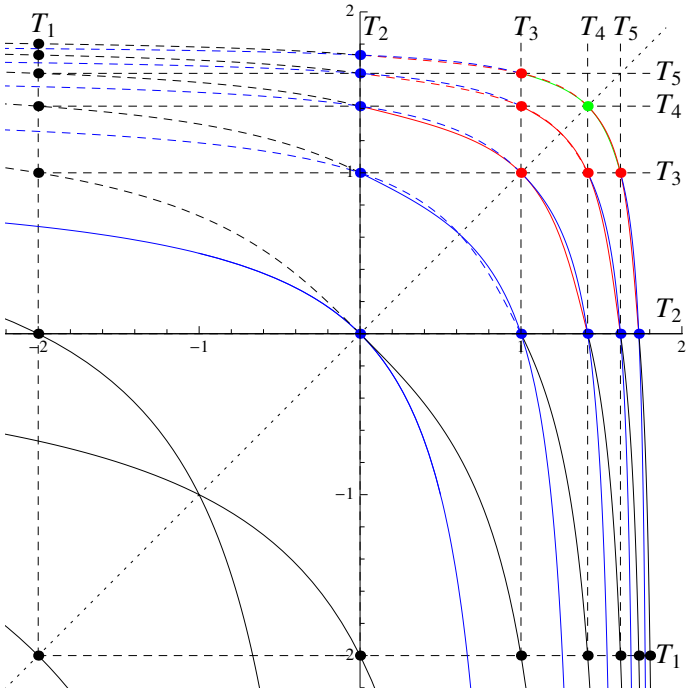

FIGURE 7. Graph of the lines $\mathcal{T}_{p,q}$ and points $P_{p,q}$ for $2 \leqslant p+q \leqslant 8$, using a color code according to the lower index p or q. The black points correspond to the no shrinking points $P_{1,q}$ and $P_{p,1}$. The dashed lines are reflections of the continuum ones with respect to the diagonal $T_L = T_R$.

5. Proofs of some results

In this section, we give the proofs of some results. To simplify the notation, in what follows we write sometimes row vectors instead of column vectors when there is no danger of confusion.

We will start by introducing the auxiliary functions h^+ and h^- to be used in the following. Any point $\mathbf{x}_0 = (x_0, y_0)$ of the ray Π_{θ_0} when $\theta_0 \neq 0, 1/2$, see (9), can be written as $\mathbf{x}_0 = (1, \nu_0)x_0$. When $x_0 > 0$ and $T_R \neq \nu_0$, we have

$$\mathbf{G}(\mathbf{x}_0) = \begin{pmatrix} T_R - \nu_0 \\ 1 \end{pmatrix} x_0 = \begin{pmatrix} 1 \\ (T_R - \nu_0)^{-1} \end{pmatrix} x_1 = \begin{pmatrix} 1 \\ \nu_1 \end{pmatrix} x_1, \tag{24}$$

where $x_1 = (T_R - \nu_0)x_0$, and we introduce the map h^+ as follows,

$$\nu_1 = h^+(\nu_0) = \frac{1}{T_R - \nu_0}, \tag{25}$$

which is locally increasing and its possible fixed points are

$$\nu_1^+ = \frac{T_R - \sqrt{T_R^2 - 4}}{2}, \quad \nu_2^+ = \frac{T_R + \sqrt{T_R^2 - 4}}{2}. \tag{26}$$

Analogously, when $x_0 < 0$ and $T_L \neq \nu_0$, we have

$$\mathbf{G}(\mathbf{x}_0) = \begin{pmatrix} T_L - \nu_0 \\ 1 \end{pmatrix} x_0 = \begin{pmatrix} 1 \\ (T_L - \nu_0)^{-1} \end{pmatrix} x_1 = \begin{pmatrix} 1 \\ \nu_1 \end{pmatrix} x_1, \tag{27}$$

where $x_1 = (T_L - \nu_0)x_0$, and we introduce the map h^- as follows,

$$\nu_1 = h^-(\nu_0) = \frac{1}{T_L - \nu_0}, \tag{28}$$

which is locally increasing and its possible fixed points are

$$\nu_1^- = \frac{T_L - \sqrt{T_L^2 - 4}}{2}, \quad \nu_2^- = \frac{T_L + \sqrt{T_L^2 - 4}}{2}. \tag{29}$$

Next, we will determine the map $\mathcal{S}$ defined in Lemma 2.2 by considering the three possible cases for the sign of x_0.

5.1. **Proof of Lemma 2.2.** Assume first that $x_0 = 0$. Since $\mathbf{G}(0, y_0) = (-y_0, 0)$, we see that the rays Π_0 and $\Pi_{1/2}$ are mapped into the rays $\Pi_{1/4}$ and $\Pi_{3/4}$ respectively, so $\mathcal{S}(0) = 1/4$ and $\mathcal{S}(1/2) = 3/4$.

Assume that $x_0 > 0$, then we have $\mathbf{x}_0 = (1, \nu_0)x_0$, where $\nu_0 = -\cot(2\pi\theta_0)$ with $0 < \theta_0 < 1/2$. Next, we study the three different cases depending on the sign of $T_R - \nu_0$. If $T_R - \nu_0 = 0$, that is, for $\theta_0 = \theta_{T_R}$ where

$$\theta_{T_R} = \frac{1}{2\pi}\cot^{-1}(-T_R), \tag{30}$$

from (24) we get $\mathbf{G}(\mathbf{x}_0) = (0, x_0)$, and so $\theta_1 = 1/2$, where we consider the branch of $\cot^{-1}(\cdot)$ that takes values in the interval $(0, \pi)$.

If $T_R - \nu_0 > 0$, then $x_1 > 0$ and $1/4 < \theta_1 < 1/2$. Hence

$$\theta_1 = \frac{1}{2\pi}\cot^{-1}\left(\frac{-1}{T_R + \cot(2\pi\theta_0)}\right) = \frac{1}{2} - \frac{1}{2\pi}\cot^{-1}\left(\frac{1}{T_R + \cot(2\pi\theta_0)}\right)$$

or equivalently

$$\theta_1 = \mathcal{S}(\theta_0) = \frac{1}{2} - \frac{1}{2\pi}\tan^{-1}\left(T_R + \cot(2\pi\theta_0)\right).$$

If $T_R - \nu_0 < 0$, then $x_1 < 0$ and $1/2 < \theta_1 < 3/4$. Hence

$$\theta_1 = \frac{1}{2} + \frac{1}{2\pi}\cot^{-1}\left(\frac{-1}{T_R + \cot(2\pi\theta_0)}\right) = \frac{1}{2} - \frac{1}{2\pi}\tan^{-1}\left(T_R + \cot(2\pi\theta_0)\right).$$

Note that this last expression unifies the three cases whichever be the sign of the expression $T_R - \nu_0 = T_R + \cot(2\pi\theta_0)$.

Assume that $x_0 < 0$, then $\mathbf{x}_0 = (1, \nu_0)x_0$, where $\nu_0 = -\cot(2\pi\theta_0)$ with $1/2 < \theta_0 < 1$. If $T_L - \nu_0 = 0$, that is, for $\theta_0 = \theta_{T_L}$ where

$$\theta_{T_L} = \frac{1}{2} + \frac{1}{2\pi}\cot^{-1}(-T_L), \tag{31}$$

from (27) we get $\mathbf{G}(\mathbf{x}_0) = (0, x_0)$, and so $\theta_1 = 0$. If $T_L - \nu_0 > 0$, that is $1/2 < \theta_0 < \theta_{T_L}$, we have $x_1 < 0$ and $1/2 < \theta_1 < 1$. Hence

$$\theta_1 = \frac{1}{2} + \frac{1}{2\pi}\cot^{-1}\left(\frac{-1}{T_L + \cot(2\pi\theta_0)}\right) = 1 - \frac{1}{2\pi}\cot^{-1}\left(\frac{1}{T_L + \cot(2\pi\theta_0)}\right)$$

or equivalently

$$\theta_1 = \mathcal{S}(\theta_0) = 1 - \frac{1}{2\pi}\tan^{-1}\left(T_L + \cot(2\pi\theta_0)\right).$$

If $T_L - \nu_0 < 0$, that is $\theta_{T_L} < \theta_0 < 1$, we have $x_1 > 0$ and $0 < \theta_1 < 1/4$. Hence

$$\theta_1 = S(\theta_0) = \frac{1}{2\pi}\cot^{-1}\left(\frac{-1}{T_L + \cot(2\pi\theta_0)}\right) = -\frac{1}{2\pi}\tan^{-1}\left(T_L + \cot(2\pi\theta_0)\right),$$

and we have shown Lemma 2.2.

5.2. **Proof of Proposition 3.1.** We look for the fixed points of the map $h = h^- \circ h^+$, where h^+ and h^- are defined in (25) and (28) respectively. Since under our hypotheses the map $\mathcal{S}$ has no fixed points, the possible fixed points of h correspond one to one with period-two orbits of map $\mathcal{S}$ whenever the map h represent the dynamics ruled by the map $\mathcal{S}$.

If $h^-(h^+(\nu)) = \nu$, then after some algebra we get the equivalent condition $T_L\nu^2 - T_RT_L\nu + T_R = 0$. This equation has the possible solutions

$$\mu_1 = \frac{T_RT_L - \sqrt{(T_RT_L)^2 - 4T_RT_L}}{2T_L}, \quad \mu_2 = \frac{T_RT_L + \sqrt{(T_RT_L)^2 - 4T_RT_L}}{2T_L}.$$

If $T_RT_L < 4$, the map h has no fixed points and statement (a) is shown.

If $T_RT_L \geqslant 4$, then under our hypotheses we must have $T_R < 0, T_L < 0$, and it is easy to see that

$$h^-(h^+(\mu_1)) = h^-\left(\frac{1}{\mu_2}\right) = \mu_1, \quad h^-(h^+(\mu_2)) = h^-\left(\frac{1}{\mu_1}\right) = \mu_2.$$

If $T_RT_L = 4$, we have $\mu_1 = \mu_2 = T_R/2 < 0$, and the map h has only one fixed point, when $T_RT_L > 4$, the map h has two fixed points.

To determine their stability, we compute the derivative h' at the above fixed points μ_1, μ_2. For $T_R T_L = 4$ we get $h'(\mu_1) = 1$, so we have a non hyperbolic fixed point. For $T_R T_L > 4$, we have

$$\mu_2 < \mu_1 < 0, \quad h'(\mu_1) = (\mu_1/\mu_2)^2 < 1, \quad h'(\mu_2) = (\mu_2/\mu_1)^2 > 1,$$

so μ_1 (μ_2) is a stable (respectively, unstable) fixed point for the map h.

Here we check that these fixed points are actually representatives of period-two orbits of the map $\mathcal{S}$. First, we will see that the period-two orbit $\{\mu_1, \mu_2^{-1}\}$ of map h leads to a periodic orbit of the map $\mathcal{S}$. It is direct to see that a point $\mathbf{x}_1 = (1, \mu_1)x$ with $x > 0$ is mapped into the point

$$\mathbf{x}_2 = \mathbf{G}(\mathbf{x}_1) = (T_R - \mu_1, 1)\, x = (\mu_2, 1)\, x = \left(1, \mu_2^{-1}\right) \mu_2 x \in \Sigma^-,$$

and the point $\mathbf{x}_2$ is mapped into $\mathbf{G}(\mathbf{x}_2) = (T_L\mu_2 - 1, \mu_2)\, x = \mu_2\mu_1^{-1}\mathbf{x}_1$. By writing $\mu_1 = -\cot(2\pi\hat{\theta}_1^+), \quad \mu_2^{-1} = -\cot(2\pi\hat{\theta}_1^-)$, with $0 < \hat{\theta}_1^+ < 1/4$ and $1/2 < \hat{\theta}_1^- < 3/4$, we have that $\mathbf{G}(\Pi_{\hat{\theta}_1^+}) = \Pi_{\hat{\theta}_1^-}$ and $\mathbf{G}(\Pi_{\hat{\theta}_1^-}) = \Pi_{\hat{\theta}_1^+}$. So the points μ_1 and μ_2^{-1} correspond to a true periodic orbit of map $\mathcal{S}$. In a similar way we can prove that the orbit $\{\mu_2, \mu_1^{-1}\}$ correspond to an unstable periodic orbit and the proof is done.

Remark 5.1. Regarding the notation in the above proof, we note that when $T^+T^- = 4$ we have $||\mathbf{x}_1|| = ||\mathbf{x}_2||$ and $\mathbf{G}(\mathbf{x_2}) = \mathbf{x}_1$, so every point on the rays $\Pi_{\hat{\theta}_1^+}$ and $\Pi_{\hat{\theta}_1^-}$ is periodic for the map $\mathbf{G}$. When $T^+T^- > 4$ we have $||\mathbf{x}_2|| > ||\mathbf{x}_1||$ and $||\mathbf{G}(\mathbf{x}_2)|| > ||\mathbf{x}_1||$, hence the dynamics on the invariant rays $\Pi_{\hat{\theta}_1^+}$ and $\Pi_{\hat{\theta}_1^-}$ related to the stable fixed points μ_1 and μ_2^{-1} are unbounded. Similarly, we can show for the orbits corresponding to the unstable fixed points μ_2, μ_1^{-1} that the dynamics on the related invariant rays tend to the origin.

5.3. **Proof of Proposition 3.2.** Before proving Proposition 3.2, we introduce the following Lemma.

Lemma 5.2. *If $p, q \geqslant 2$, and $\mathbf{u}_0 = (0, -1)$, the following statements hold for the map $\mathbf{G}$.*

(a) *Assume that $T_p \leqslant T_R < T_{p+1}$ and $\mathbf{x} = (x_0, y_0)$ where $x_0 \geqslant 0$ and $y_0 < 0$. Then we have $\mathbf{x}_k = \mathbf{G}^{(k)}(\mathbf{x}) = A(T_R)^k\mathbf{x}$ for $1 \leqslant k \leqslant p$. When $T_R = T_p$ we get $\mathbf{G}^{(p)}(\mathbf{x}) = -\mathbf{x}$ and when $T_p < T_R < T_{p+1}$, we get $\mathcal{L}^{(p)}(0) < 1/2 < \mathcal{L}^{(p+1)}(0)$, and so the sequence $A(T_R)^{p+1}$ is admissible for the point $\mathbf{u}_0$.*

(b) *Assume that $T_{q-1} < T_L \leqslant T_q$ and $\mathbf{x} = (x_0, y_0)$ with $x_0 \leqslant 0, y_0 > 0$. Then we have $\mathbf{G}^{(k)}(\mathbf{x}) = A(T_L)^k\mathbf{x}$ for $1 \leqslant k \leqslant q-1$. When $T_L = T_q$ we get $\mathbf{G}^{(q)}(\mathbf{x}) = -\mathbf{x}$ and when $T_{q-1} < T_L < T_q$, we*

get $\mathcal{L}^{(q-1)}(1/2) < 1 < \mathcal{L}^{(q)}(1/2)$, *and so the sequence* $A(T_L)^q$ *is admissible for the point* $-\mathbf{u}_0$.

(c) *If* $T_p \leqslant T_R < T_{p+1}$ *and* $T_{q-1} < T_L \leqslant T_q$, *then the matrix* $A(T_L)^{q-1}A(T_R)^{p+1}$ *is admissible for the point* $\mathbf{u}_0$ *and the matrix* $A(T_R)^pA(T_L)^q$ *is admissible for the point* $-\mathbf{u}_0$.

Proof. When $T_p \leqslant T_R < T_{p+1}$, by writing $T_R = 2\cos\alpha$ we have

$$2\cos\left(\frac{\pi}{p}\right) \leqslant 2\cos\alpha < 2\cos\left(\frac{\pi}{p+1}\right),$$

which implies $\pi/(p+1) < \alpha \leqslant \pi/p$, and so $\sin(p+1)\alpha < 0 \leqslant \sin p\alpha$.

If $\mathbf{x} = (x, y)$ with $x \geqslant 0, y < 0$, from Proposition A.2 (b), the first coordinate of $\mathbf{x}_k{=}A(T_R)^k\mathbf{x}$ is

$$x_k = \frac{x\sin((k+1)\alpha) - y\sin k\alpha}{\sin\alpha}. \tag{32}$$

Then for $1 \leqslant k \leqslant p-1$, we have $x_k > 0$, and so $\mathbf{x}_k = \mathbf{G}^{(k)}\mathbf{x} = A(T)^k\mathbf{x}$ for $1 \leqslant k \leqslant p$. When $T_R = T_p$, we have $A(T_p)^p = -I$, and then $\mathbf{x}_p = -\mathbf{x}$. When $T_p < T_R < T_{p+1}$ and $\mathbf{x} = \mathbf{u}_0$, from (32) we have

$$x_p = \frac{\sin p\alpha}{\sin\alpha} > 0, \quad x_{p+1} = \frac{\sin(p+1)\alpha}{\sin\alpha} < 0,$$

and statement(a) follows.

The proof of statement (b) is similar to the proof of statement a).

If $T_p \leqslant T_R < T_{p+1}$, from statement (a) we get

$$\mathbf{G}^{(p+1)}(\mathbf{u}_0) = A(T_R)^{p+1}\mathbf{u}_0 \in \Sigma^-.$$

If in addition $T_{q-1} < T_L \leqslant T_q$, from statement (b), we obtain that the sequence $A(T_L)^{q-1}$ is admissible for the point $A(T_R)^{p+1}\mathbf{u}_0$, and so

$$\mathbf{G}^{(p+q)}(\mathbf{u}_0) = A(T_L)^{q-1}A(T_R)^{p+1}\mathbf{u}_0.$$

If $T_{q-1} < T_L \leqslant T_q$, from statement (b), we get

$$\mathbf{G}^{(q)}(-\mathbf{u}_0) = A(T_L)^q(-\mathbf{u}_0) \in \Sigma^+.$$

If in addition If $T_p \leqslant T_R < T_{p+1}$, from statement (a) we obtain that $A(T_R)^p$ is admissible for the point $A(T_L)^q(-\mathbf{u}_0)$, and so

$$\mathbf{G}^{(p+q)}(-\mathbf{u}_0) = A(T_R)^pA(T_L)^q(-\mathbf{u}_0),$$

and statement (c) is proven. □

Next we prove Proposition 3.2, where it is assumed $T_R = T_p$ and $T_L = T_q$. Since the map S is increasing with respect the variable θ and $\mathbf{G}^{(p+1)}(\mathbf{u}_0) \in \Sigma^-$, the iterates of every point in Σ^+ eventually enter the

zone Σ^-. More precisely, if $\mathbf{x} = (x, y) \in \Sigma^+$ and $\mathbf{G}(\mathbf{x}) \in \Sigma^-$, then $\mathbf{G}(\mathbf{x}) \in \Omega^-$ where

$$\Omega^- = \{\mathbf{x} = (x, y) \in \mathbb{R}^2 : x \leqslant 0, y > 0\}.$$

Similarly, since $\mathbf{G}^{(q+1)}(-\mathbf{u}_0) \in \Sigma^+$, we can assure that the iterates of every point in Σ^- eventually enter the zone Σ^+. More precisely, if $\mathbf{x} = (x, y) \in \Sigma^-$ and $\mathbf{G}(\mathbf{x}) \in \Sigma^+$, then $\mathbf{G}(\mathbf{x}) \in \Omega^+ = \{\mathbf{x} = (x, y) \in \mathbb{R}^2 : x \geqslant 0, y < 0\}$, and so the orbit of every point visits the set Ω^+. Then, it is enough to show that the points of the set Ω^+ are period-$(p+q)$. If $\mathbf{x} \in \Omega^+$, from Lemma 5.2 (a) we have $\mathbf{G}^{(p)}(\mathbf{x}) = -\mathbf{x}$, and from Lemma 5.2 (b) we have $\mathbf{G}^{(q)}(-\mathbf{x}) = \mathbf{x}$ for every point in the set Ω^- and the proof is done.

5.4. **Proof of Proposition 3.6.** Statements (a) and (b) are direct. Statement (c) follows from Remark 3.5 and statement (b).

In order to prove statement (d) let us consider the function

$$g(T_R, T_L) = \mathcal{L}_{\mathcal{S}}^{(p+q)}(0; T_R, T_L),$$

where $\mathcal{L}_{\mathcal{S}}^{(p+q)}$ is the $p+q$ iterate of the lift $\mathcal{L}_{\mathcal{S}}$ defined in (12). From Remark 2.3, the map $\mathcal{S}$ and its corresponding lift are decreasing with respect to both parameters T_L, T_R, and noting that

$$g(T_p, T_q) = g(T_{p+1}, T_{q-1}) = 1,$$

we have $g(T_R, T_{q-1}) > 1$ and $g(T_R, T_q) < 1$ for $T_p < T_R < T_{p+1}$. Take now T_R as a fixed value in the interval (T_p, T_{p+1}) and introduce the function $h(T_L) = g(T_R, T_L)$. This function h is decreasing because the map $\mathcal{S}$ is decreasing with respect to both parameters T_L and T_R, and verifies $h(T_q) < 1 < h(T_{q-1})$, so there exists only one value $\widehat{T}_L$ with $T_{q-1} < \widehat{T}_L < T_q$ such that $h(\widehat{T}_L) = g(T_R, \widehat{T}_L) = 1$, for every T_R in the interval (T_p, T_{p+1}). Then, there exists only one function $T_L = \mathcal{T}_{p,q}^B(T_R)$, defined for T_R in the interval (T_p, T_{p+1}) satisfying $T_{q-1} < \mathcal{T}_{p,q}^B(T_R) < T_q$, and $g(T_R, \mathcal{T}_{p,q}^B(T_R)) = \mathcal{L}_{\mathcal{S}}^{(p+q)}(0; T_R, \mathcal{T}_{p,q}^B(T_R)) = 1$. Hence the map $\mathcal{S}$ has two periodic orbits on the graph of the function $\mathcal{T}_{p,q}^B$.

From Proposition 3.4 we see that the function $\mathcal{T}_{p,q}^B$ is implicitly defined for the equation $\mathcal{F}_{p,q}(T_R, T_L) = 0$, see (18). Then From Remark A.3 and Lemma A.4 in Appendix A, the computation of the first derivatives at the point $P_{p,q}$ and $P_{p+1,q-1}$ are straightforward and the proof is done.

5.5. **Proof of Proposition 3.9.** We prove the existence of the function $\mathcal{T}_{p,q}$ by using the Intermediate Value Theorem. Firstly, we will compare the values of the function $\mathbb{T}_{p,q}$ on the segment

$$\Gamma_1 = \{(T_R, T_L) : T_R = T_p,\ T_{q-1} < T_L < T_q\}$$

with the ones on the graph of the function $\mathcal{T}^B_{p,q}(T_L)$ for $T_p < T_L < T_{p+1}$. Secondly, we will consider the values of $\mathbb{T}_{p,q}$ on the segment

$$\Gamma_2 = \{(T_R, T_L) : T_R = T_p,\ T_q < T_L < T_{q+1}\},$$

and on the graph of the function $\mathcal{T}^B_{p-1,q+1}(T_L)$ for $T_{p-1} < T_L < T_p$.

For points (T_L, T_R) on Γ_1, by putting $T_L = 2\cos(\alpha)$ we get

$$T_{q-1} = 2\cos\left(\frac{\pi}{q-1}\right) < 2\cos(\alpha) < 2\cos\left(\frac{\pi}{q}\right) = T_q,$$

implying $\pi < q\alpha < q\pi/(q-1)$. Then, for $q \geqslant 3$ we have $\pi < q\alpha < 3\pi/2$, and from Remark A.3 in Appendix A we get,

$$\mathbb{T}_{p,q}(T_p, 2\cos(\alpha)) = \Psi_{q-1}(2\cos(\alpha)) - \Psi_{q+1}(2\cos(\alpha)) = -2\cos(q\alpha).$$

Hence, for points on the segment Γ_1 we have $0 < \mathbb{T}_{p,q}(T_p, T_L) < 2$.

For points (T_L, T_R) on the graph of the function $\mathcal{T}^B_{p,q}(T_R)$, we have

$$\mathbb{T}_{p,q}(T_R, T_L) = \operatorname{trace}(A(T_L)^q A(T_R)^p) = \lambda + \frac{1}{\lambda},$$

where $\lambda = \Psi_{q+1}(T_L)\Psi_{p+1}(T_R) - \Psi_q(T_L)\Psi_p(T_R)$. Due to the facts that $\mathbb{T}_{p,q}$ is a continuous function with $\mathbb{T}_{p,q}(T_p, T_q) = 2$, we conclude that $\lambda > 0$. Then $\mathbb{T}_{p,q}(T_R, T_L) \geqslant 2$ with $\mathbb{T}_{p,q}(T_R, T_L) = 2$ only when $\lambda = 1$. Although $\lambda = 1$ is a eigenvalue of the matrix $A(T_L)^q A(T_R)^p$ when $(T_R, T_L) = (T_p, T_q)$, we can ensure that the eigenvalues of the matrix $A(T_L)^q A(T_R)^p$ are greater than one in the remain points on the graph of the function $\mathcal{T}^B_{p,q}$. Otherwise, our map would have a $\mathcal{B}^0$ periodic orbit on the quoted graph that is not possible according to Proposition 3.4.

Consequently, for every fixed value T_L with $T_{q-1} < T_L < T_q$ there exists a value $\widehat{T}_R$ with $T_p < \widehat{T}_R < T_{p+1}$ such that $\mathbb{T}_{p,q}(\widehat{T}_R, T_L) = 2$, and taking into account that the lift is decreasing with respect to the parameters, we have that the value $\widehat{T}_R$ is unique. Moreover, we can define a monotone function $h(T_L)$ on the interval (T_{q-1}, T_q) with values on the interval (T_p, T_{p+1}), such that $\mathbb{T}_{p,q}(h(T_L), T_L) = 2$. Taking into account that $\mathbb{T}_{p,q}(T_p, T_q) = \mathbb{T}_{p,q}(T_{p+1}, T_{q-1}) = 2$, we can extend the function by puting $T_p = h(T_q)$ and $T_{p+1} = h(T_{q-1})$. Hence, the inverse function $h^{-1} = \mathcal{T}_{p,q}$ exists which is defined on the interval $[T_p, T_{p+1}]$ and its domaine is $[T_{q-1}, T_q]$, such that $\mathbb{T}_{p,q}(T_R, \mathcal{T}_{p,q}(T_R)) = 2$

Following a similar procedure by considering the values of $\mathbb{T}_{p,q}$ on the segment Γ_2 and on the graph of $\mathcal{T}^B_{p-1,q+1}(T_L)$ for $T_{p-1} < T_L < T_p$, we

can continuously prolongate the above function to the interval $[T_{p-1}, T_p]$ with values on the interval $[T_q, T_{q+1}]$.

Then, we have defined a function $\mathcal{T}_{p,q}$ defined on the interval $[T_{p-1}, T_{p+1}]$ whose domaine is the interval $[T_{q-1}, T_{q+1}]$ such that at the non shrinking points on its graph our map has only one periodic orbit.

To prove the local expansions (20) and (22), we implicitly differentiate the equality $\mathbb{T}_{p,q}(T_R, T_L) - 2 = 0$, and we obtain

$$\frac{\partial \mathbb{T}_{p,q}}{\partial T_R} + \frac{\partial \mathbb{T}_{p,q}}{\partial T_L}\frac{dT_L}{dT_R} = 0.$$

Taking into account Remark A.3 and Lemma A.4 in Appendix A we compute the partial derivatives at the two points $P_{p-1,q+1}$ and $P_{p+1,q-1}$ and the expressions (20) and (22) follow.

The proof of expansion (21) is slightly different because the gradient of the function $\mathbb{T}_{p,q}$ at the point $P_{p,q}$ vanishes, see Lemma A.4. Then, by differentiating once more time we get

$$\frac{\partial^2 \mathbb{T}_{p,q}}{\partial T_R^2} + 2\frac{\partial^2 \mathbb{T}_{p,q}}{\partial T_L \partial T_R}\frac{dT_L}{dT_R} + \frac{\partial^2 \mathbb{T}_{p,q}}{\partial T_L^2}\left(\frac{dT_L}{dT_R}\right)^2 + \frac{\partial \mathbb{T}_{p,q}}{\partial T_L}\frac{d^2T_L}{dT_R^2} = 0. \tag{33}$$

Since the point $P_{p,q}$ is a singular point, the equality (33) reduces to the quadratic form in dT_L/dT_R,

$$\frac{2p^2}{T_p^2 - 4} + \frac{4pq(T_pT_q - 4)}{(T_p^2 - 4)(T_q^2 - 4)}\frac{dT_L}{dT_R} + \frac{2q^2}{T_q^2 - 4}\left(\frac{dT_L}{dT_R}\right)^2 = 0$$

By applying bifurcation theory around this ramification point, see [9], we conclude the existence of two branches of points with slopes at the point $P_{p,q}$,

$$\frac{dT_L^a}{dT_R} = -\frac{p(T_q - 2)}{q(T_p - 2)} \quad \text{and} \quad \frac{dT_L^b}{dT_R} = -\frac{p(T_q + 2)}{q(T_p + 2)}.$$

Thus, at the point $P_{p,q}$ we have the following inequalities,

$$\frac{dT_L^a}{dT_R} < \frac{d\mathcal{T}_{p,q}^B}{dT_R} < \frac{dT_L^b}{dT_R} < 0.$$

Therefore, for $T_R > T_p$, the graph of the function T_L^b is locally above the graph of the function $\mathcal{T}_{p,q}^B$. Since from Remark 3.7 the matrix $A(T_L)^q A(T_R)^p$ represents the map $\mathbf{G}^{(p+q)}$ only for points (T_R, T_L) with $T_R > T_p$ and located below the graph of the function $\mathcal{T}_{p,q}^B$, we conclude that the function T_L^b does not represent the dynamical behavior of the map $\mathbf{G}^{(p+q)}$, so we identify T_L^a with the function $\mathcal{T}_{p,q}$ and (21) follows.

To prove statement (b), we solve the equation $\mathbb{T}_{p,2}(T_R, T_L) = 2$ for the variable T_L. By using the relation $\Psi_n^2 = \Psi_{n+1}\Psi_{n-1} + 1$, which can be easily proved by induction, we obtain $T_L = \mathcal{T}_{p,2}^{\pm}(T_R)$, where

$$\mathcal{T}_{p,2}^{\pm}(T_R) = \frac{\Psi_p^+ \pm \sqrt{(\Psi_p^+)^2 - \Psi_{p+1}^+(\Psi_{p-1}^+ - \Psi_{p+1}^+ - 2)}}{\Psi_{p+1}^+} = \frac{\Psi_p^+ \pm (\Psi_{p+1}^+ + 1)}{\Psi_{p+1}^+},$$

where Ψ_n^+ stands for $\Psi_n(T_R)$. Then, the function $\mathcal{T}_{p,2}^+$ is the predicted function $\mathcal{T}_{p,2}$ and the proof of statement (b) is done.

Statement (c) is direct.

5.6. **Proof of Proposition 2.5.** (a) If either $T_R \geqslant 2$ or $T_L \geqslant 2$, then from (26) or (29) follows that the map $\mathcal{S}$ has at least a fixed point and then directly we get $\rho = 0$.

(b) According to Proposition 3.1, the map $\mathcal{S}$ has two period-two orbits, and then directly follows $\rho = 1/2$.

(c) Since the rotation number is invariant under conjugation, to compute the rotation number of $\mathcal{S}$ we will compute the rotation number of a conjugate map. When $T_R = 2\cos(2\pi\alpha)$ and $T_L = 2\cos(\pi/q)$, we make the conjugation $\mathbf{x}_n = M\mathbf{y}_n$, where

$$M = \begin{pmatrix} 1 & 0 \\ \cos(2\pi\alpha) & \sin(2\pi\alpha) \end{pmatrix},$$

and we obtain the conjugate map $\mathbf{y}_{n+1} = \mathbf{R}(\mathbf{y}_n)$ where

(34)

$$\mathbf{R}(\mathbf{y}_n) = \begin{cases} R^-\mathbf{y}_n = M^{-1}\begin{pmatrix} 2\cos(\pi/q) & -1 \\ 1 & 0 \end{pmatrix} M\mathbf{y}_n, & \text{if } \mathbf{y}_n \in \Sigma^- \bigcup \Sigma, \\ \\ R^+\mathbf{y}_n = \begin{pmatrix} \cos(2\pi\alpha) & -\sin(2\pi\alpha) \\ \sin(2\pi\alpha) & \cos(2\pi\alpha) \end{pmatrix}\mathbf{y}_n, & \text{if } \mathbf{y}_n \in \Sigma^+. \end{cases}$$

To determine the rotation number we consider a lift $\mathcal{L}_r$ of the map (34) and take a point $\mathbf{y}$ belonging to the ray Π_θ, where $\theta \in (1/2, 3/4)$. From Lemma 5.2 we know that $(R^-)^q\mathbf{y} = -\mathbf{y}$ and so $\mathcal{L}_r^{(q)}(\theta) = \theta + 1/2$. Moreover, since R^+ represents a rigid rotation, a minimum integer number n_1 exists such that

$$\mathcal{L}_r^{(n_1+q)}(\theta) = \theta_1 > 1 + \frac{1}{2}.$$

Also, a minimum integer number n_2 exists such that

$$\mathcal{L}_r^{(n_2+q)}(\theta_1) = \mathcal{L}_r^{((n_2+q)+(n_1+q))}(\theta) = \theta_2 > 2 + \frac{1}{2}.$$

By repeating the process, we can assure that a minimum integer n_p exists with

$$\mathcal{L}_r^{(n_p+q)}(\theta_{p-1}) = \mathcal{L}_r^{((n_p+q)+\cdots+(n_1+q))}(\theta) = \theta_p > p + \frac{1}{2}.$$

By calling $n_1 + n_2 + \cdots + n_p = k$, we have $p = \lfloor 2\alpha k \rfloor$ and so

$$(n_1 + q) + \cdots + (n_p + q) = k + \lfloor 2\alpha k \rfloor q, \quad \theta_p = \theta_0 + k\alpha + \lfloor 2k\alpha \rfloor/2.$$

Hence,

$$\rho(\theta) = \lim_{n\to\infty} \frac{\mathcal{L}_r^{(n)}(\theta)}{n} = \lim_{k\to\infty} \frac{\theta_p}{(n_1 + q) + \cdots + (n_p + q)} = \frac{2\alpha}{1 + 2\alpha q}.$$

(d) To compute the rotation number we consider the orbit of a point $\mathbf{x}_0 = (x_0, y_0)$, where $x_0 \leqslant 0$ and $y_0 < 0$. Firstly, we show that for $1 \leqslant k < n$ the sequences $(A^+A^-)^k$ and $A^-(A^+A^-)^k$ are admissible to compute $\mathbf{G}^{(2k)}(\mathbf{x}_0)$ and $\mathbf{G}^{(2k+1)}(\mathbf{x}_0)$ respectively, that is

$$\mathbf{x}_{2k} = (A^+A^-)^k\mathbf{x}_0, \quad \mathbf{x}_{2k+1} = A^-(A^+A^-)^k\mathbf{x}_0. \tag{35}$$

Since $(A^+A^-)^k = MD^kM^{-1}$, where

$$M = \begin{pmatrix} a & a \\ 1 + e^{i\frac{\pi}{n}} & 1 + e^{-i\frac{\pi}{n}} \end{pmatrix}, \quad D = \begin{pmatrix} e^{-i\frac{\pi}{n}} & 0 \\ 0 & e^{i\frac{\pi}{n}} \end{pmatrix}$$

we obtain

$$(A^+A^-)^k = \begin{pmatrix} \dfrac{\sin k\omega_{2n} + \sin(k+1)\omega_{2n}}{\sin\omega_{2n}} & -\dfrac{T_R \sin k\omega_{2n}}{\sin\omega_{2n}} \\ \dfrac{2\,(1+\cos\omega_{2n})\sin k\omega_{2n}}{T_R \sin\omega_{2n}} & -\dfrac{\sin\ k\omega_{2n} + \sin(k-1)\omega_{2n}}{\sin\omega_{2n}} \end{pmatrix},$$

and $A^-(A^+A^-)^k$ is the matrix

$$\begin{pmatrix} \dfrac{2\,(1+\cos\omega_{2n})\sin(k+1)\omega_{2n}}{T_R \sin\omega_{2n}} & -\dfrac{\sin(k+1)\omega_{2n} + \sin k\omega_{2n}}{\sin\omega_{2n}} \\ \dfrac{\sin k\omega_{2n} + \sin(k+1)\omega_{2n}}{\sin\omega_{2n}} & -\dfrac{T_R \sin k\omega_{2n}}{\sin\omega_{2n}} \end{pmatrix}.$$

Then for $1 \leqslant k \leqslant n-1$, we have

$$x_{2k} = \frac{\sin k\omega_{2n} + \sin(k+1)\omega_{2n}}{\sin\omega_{2n}} x_0 - \frac{T_R \sin k\omega_{2n}}{\sin\omega_{2n}} y_0 \leqslant 0,$$

$$x_{2k+1} = \frac{2\,(1+\cos\omega_{2n})\sin(k+1)\omega_{2n}}{T_R \sin\omega_{2n}} x_0 - \frac{\sin(k+1)\omega_{2n} + \sin k\omega_{2n}}{\sin\omega_{2n}} y_0 \geqslant 0,$$

so relationship (35) is true. Moreover, since $(A^+A^-)^n = -I$, we get $\mathbf{G}^{(2n)}(\mathbf{x}_0) = -\mathbf{x}_0$.

Similarly, we can see that for $1 \leqslant k \leqslant n-1$,

$$\mathbf{x}_{2n+2k} = (A^-A^+)^k(-\mathbf{x}_0), \quad \mathbf{x}_{2n+2k+1} = A^+(A^-A^+)^k(-\mathbf{x}_0),$$

and it is easy deduce that

$$\mathbf{G}^{(4n)}(\mathbf{x}_0) = \mathbf{G}^{(2n)}(\mathbf{G}^{(2n)}(\mathbf{x}_0)) = \mathbf{G}^{(2n)}(-\mathbf{x}_0) = \mathbf{x}_0.$$

Finally, If r is a lift of our map, noting that $r^{(4n)}(0) = 2n-1$, we get

$$\rho = \lim_{p\to\infty} \frac{r^p(0)}{p} = \lim_{k\to\infty} \frac{r^{(4nk)}(0)}{4nk} = \lim_{k\to\infty} \frac{(2n-1)k}{4nk} = \frac{2n-1}{4n}.$$

6. Acknowledgements

Authors are partially supported by the Spanish Ministerio de Ciencia y Tecnologia, Plan Nacional I+D+I, in the frame of projects DPI2013-47293-R, MTM2012-31821 and MTM2015-65608-P, and by the Consejería de Economia-Innovacion-Ciencia-Empleo de la Junta de Andalucía under grant P12-FQM-1658.

References

1. A. Andronov, A. Vitt and S. Khaikin, "Theory of Oscillations" Pergamon Press, Oxford, 1966.
2. V. Avrutin, A. Granados and M. Schanz, Sufficient conditions for a period incrementing big bang bifurcation in one-dimensional maps, Nonlinearity **24** (2011), 2575–2598.
3. Banerjee S and Grebogi C, Border collision bifurcations in two-dimensional piecewise smooth maps, Phys. Rev. E **59** (1999), 4052–61.
4. M. di Bernardo, C.J. Budd, A. R. Champneys, P. Kowalczyk, "Piecewise-Smooth Dynamical Systems: Theory and Applications", Appl. Math. Sci., vol 163, Springer-Verlag London Ltd., London, 2008.
5. S. Falcon and A. Plaza, On k-Fibonacci sequences and polynomials and their derivatives, Chaos, Solitons and Fractals **39** (2009), 1005–1019.
6. J. Guckenheimer, P.Holmes, "Nonlinear Oscillations, Dynamical Systems and Bifurcations of Vector Fields," Springer Verlag, New York, 1983.
7. M. Henon, A two-dimensional mapping with a strange attarctor, Communications in Mathematical Physics **50** (1976), 69–77.
8. V. E. Hoggart Jr. and C. T. Long, Divisibility Properties of Generalized Fibonacci Polynomials, Fibonacci Quarterly, **12** (1974), 113–120.
9. H. B. Keller, "Numerical Solution of Bifurcation and Nonlinear Eigenvalue Problems." Applications of Bifurcation Theory, pp 359-384, Academic Press, New York, 1977.
10. J. C. Lagarias and E. Rains, Dynamics of a Family of Piecewise-Linear Area-preserving Plane Maps I. Rational Rotation Numbers, Journal Difference Equations and Applications **11** (2005), 1089–1108.

11. J. C. Lagarias and E. Rains, Dynamics of a Family of Piecewise-Linear Area-preserving Plane Maps II. Invariant circles, Journal Difference Equations and Applications **11** (2005), 1089–1108.
12. J. C. Lagarias and E. Rains, Dynamics of a Family of Piecewise-Linear Area-preserving Plane Maps III. Cantor set spectra, Journal Difference Equations and Applications **11** (2005), 1089–1108.
13. R. Lozi , Un attracteur etrange du type Henon, Journal Physics **39** (1978), 9–10.
14. H. E. Nusse and J. A. Yorke, Border-collision bifurcation including "period two to period three" for piecewise smooth systems, Physica D **57** (1992), 39–57.
15. D.J.W. Simpson and J.D. Meiss, Shirinking point bifurcations of resonance tongues for piecewise smooth continuous map, Nonlinearity. **22** (2009), 1123–1144.
16. W.M Yang and B.L. Hao, How the Arnold's tongues become sausages in a piecewise linear circle map, Commun. Theor. Phys. **8** (1987), 1–15.

Appendix A. Generalized Fibonacci polynomials and power of matrices.

The generalized Fibonacci polynomials were introduced in [8] as,

$$u_n(x,y) = xu_{n-1}(x,y) + yu_{n-2}(x,y), \quad u_0(x,y) = 0, u_1(x,y) = 1. \tag{36}$$

By using induction we can prove prove that

$$u_n(x,y) = \frac{\sigma^n - (-y)^n\sigma^{-n}}{\sigma + y\sigma^{-1}}, \quad \text{where} \quad \sigma(x,y) = \frac{x - \sqrt{x^2+4y}}{2}.$$

In the same spirit as that in Proposition 13 in [5], we obtain the derivative of u_n with respect to the variable x as

$$u_n'(x,y) = \frac{(n-1)xu_n + 2nyu_{n-1}}{x^2+4y} = \frac{2nu_{n+1} - (n+1)xu_n}{x^2+4y} \tag{37}$$

Now, we are in position of give explicit expressions for the powers of a 2×2 matrix. First let us introduce the family of polynomials, closely related to the Fibonacci generalized polynomials, defined by the recursion

$$v_n(x,y) = xv_{n-1}(x,y) + yv_{n-2}(x,y), \quad v_0(x,y) = \beta, \quad v_1(x,y) = \alpha \tag{38}$$

By induction it is direct to show that

$$v_n(x,y) = \alpha u_n(x,y) + \beta y u_{n-1}(x,y). \tag{39}$$

Proposition A.1. *If we denote by T and D the trace and the determinant of the 2×2 matrix $A = (a_{ij})$, and $u_k = u_k(T, -D)$ the $k-$degree Fibonacci generalized polynomial, then*

$$A^n = \begin{pmatrix} a_{11}u_n - Du_{n-1} & a_{12}u_n \\ a_{21}u_n & a_{22}u_n - Du_{n-1} \end{pmatrix}.$$

Proof. From the Cayley Hamilton Theorem we have $A^n = TA^{n-1} - DA^{n-2}$. for $n \geqslant 2$. Then the entries of the matrix $A^n = (a_{ij}^{(n)})$, satisfy the recursion

$$a_{ij}^{(n)} = Ta_{ij}^{(n-1)} - Da_{ij}^{(n-2)} \quad \text{with} \quad \begin{array}{ll} a_{11}^{(0)} = 1, & a_{11}^{(1)} = a_{11}, \\ a_{12}^{(0)} = 0, & a_{12}^{(1)} = a_{12}, \\ a_{21}^{(0)} = 0, & a_{21}^{(1)} = a_{21}, \\ a_{22}^{(0)} = 1, & a_{22}^{(1)} = a_{22}. \end{array}$$

and from (38) and (39) the conclusion follows. □

Next we consider some results about the powers of the matrix

$$A(T) = \begin{pmatrix} T & -1 \\ 1 & 0 \end{pmatrix}. \tag{40}$$

In order to facilitate the study we introduce the function

$$\Psi_n(T) = u_n(T, -1), \tag{41}$$

where $u_n(x, y)$ is the generalized Fibonacci polynomial, that is

$$u_{n+1}(x, y) = xu_n(x, y) + yu_{n-1}(x, y), \quad \text{with} \quad u_0(x, y) = 0, u_1(x, y) = 1.$$

Obviously, we have

$$\Psi_{n+1}(T) = T\Psi_n(T) - \Psi_{n-1}(T), \quad \text{with} \quad \Psi_0(T) = 0, \quad \Psi_1(T) = 1.$$

Moreover, from Corollary 10 in [8], we easily deduce that

$$\Psi_n(T) = \prod_{k=1}^{n-1} \left(T - 2\cos\left(\frac{k\pi}{n}\right)\right) \tag{42}$$

Proposition A.2. *The followings statements hold for the matrix* (40).

(a) *By using the function* $\Psi_n(T)$ *defined in* (41) *we have*

$$A^n(T) = \begin{pmatrix} \Psi_{n+1}(T) & -\Psi_n(T) \\ \Psi_n(T) & -\Psi_{n-1}(T) \end{pmatrix},$$

(b) *If* $|T| < 2$, *we can put* $T = 2\cos\alpha$ *with* $0 < \alpha < \pi$, *and then*

$$A^n(2\cos\alpha) = \frac{1}{\sin\alpha} \begin{pmatrix} \sin(n+1)\alpha & -\sin n\alpha \\ \sin n\alpha & -\sin(n-1)\alpha \end{pmatrix},$$

(c) *If* $|T| > 2$, *we can put* $T = 2\gamma\cosh\alpha$ *with* $\alpha \in \mathbb{R}, \gamma = \pm 1$ *and then*

$$A^n(2\gamma\cosh\alpha) = \frac{\gamma^n}{\sinh\alpha} \begin{pmatrix} \sinh(n+1)\alpha & -\gamma\sinh n\alpha \\ \gamma\sinh n\alpha & -\sinh(n-1)\alpha \end{pmatrix}.$$

(d) *If* $|T| = 2$, *we can put* $T = 2\gamma$ *with* $\gamma = \pm 1$ *and then*

$$A^n(2\gamma) = \gamma^n \begin{pmatrix} n+1 & -\gamma n \\ \gamma n & -(n-1) \end{pmatrix}.$$

Proof. (a) The statement follows from Proposition A.1 by taking

$$a_{11} = T, \quad a_{12} = -1, \quad a_{21} = 1, \quad a_{22} = 0,$$

and using the function $\Psi_n(T)$, see (41).

(b) If $T = 2\cos\alpha = e^{i\alpha} + e^{-i\alpha}$, then $A^n = MD^nM^{-1}$ where

$$M = \begin{pmatrix} 1 & 1 \\ e^{i\alpha} & e^{-i\alpha} \end{pmatrix} \text{ and } D = \begin{pmatrix} e^{-i\alpha} & 0 \\ 0 & e^{i\alpha} \end{pmatrix},$$

and the statement is straightforward.

(c) If $T = 2\gamma\cosh\alpha$, then $A^n = MD^nM^{-1}$ where

$$M = \begin{pmatrix} 1 & 1 \\ \gamma e^{-\alpha} & \gamma e^{\alpha} \end{pmatrix} \text{ and } D = \begin{pmatrix} \gamma e^{\alpha} & 0 \\ 0 & \gamma e^{-\alpha} \end{pmatrix},$$

and the statement follows.

Statement (d) can be easily proved by induction. □

Remark A.3. As a by-product of Proposition A.2 we get for $\gamma = \pm 1$,

$$\Psi_n(2\cos\alpha) = \frac{\sin n\alpha}{\sin\alpha}, \quad \Psi_n(2\gamma\cosh\alpha) = \frac{\gamma^{n+1}\sinh n\alpha}{\sinh\alpha}, \quad \Psi_n(2\gamma) = \gamma^{n+1}n.$$

In addition, by using the notations

$$T_n = 2\cos\left(\frac{\pi}{n}\right), \quad \widehat{T}_n = T_{n-\frac{1}{2}} = 2\cos\left(\frac{\pi}{n-\frac{1}{2}}\right) \tag{43}$$

we have

$$\Psi_{n-1}(T_n) = 1, \qquad \Psi_n(T_n) = 0, \qquad \Psi_{n+1}(T_n) = -1$$

$$\Psi_{2n-2}\left(\widehat{T}_n\right) = -1, \quad \Psi_{2n-1}\left(\widehat{T}_n\right) = 0, \quad \Psi_{2n}\left(\widehat{T}_n\right) = 1.$$

and so, $\quad A^n(T_n) = -I, \quad A^{2n-1}\left(\widehat{T}_n\right) = I.$

The proof of the following lemmata is direct from expression 37 and Remark A.3.

Lemma A.4. *The two first derivatives of the function* $\Psi_n(x)$, $n \geqslant 2$, *are*

$$\Psi_n'(x) = \frac{2n\Psi_{n+1}(x) - (n+1)x\Psi_n(x)}{x^2-4},$$

$$\Psi_n''(x) = \frac{2n\Psi_{n+1}'(x) - (n+1)\Psi_n(x) - (n+3)x\Psi_n'(x)}{x^2-4}. \tag{44}$$

In particular, we have

$$\Psi'_{n-1}(T_n) = \Psi'_{n+1}(T_n) = \frac{-nT_n}{T_n^2-4}, \quad \Psi'_n(T_n) = \frac{-2n}{T_n^2-4},$$

and

$$\Psi''_n(T_n) = \frac{6nT_n}{(T_n^2-4)^2}, \quad \Psi''_{n\pm1}(T_n) = \frac{n(T_n^2+8) \mp n^2(T_n^2-4)}{(T_n^2-4)^2}.$$

The next lemmata deals with the values of some functions Ψ_k and its derivatives at the point $\widehat{T}_n$.

Lemma A.5. *The values of the functions $\Psi_{n-2}, \Psi_{n-1}, \Psi_n, \Psi_{n+1}$, at the point $\widehat{T}_n$ are,*

(45)

$$\Psi_{n-1}(\widehat{T}_n) = -\Psi_n(\widehat{T}_n) = \frac{1}{\sqrt{2+\widehat{T}_n}}, \ \Psi_{n-2}\left(\widehat{T}_n\right) = -\Psi_{n+1}(\widehat{T}_n) = \frac{1+\widehat{T}_n}{\sqrt{2+\widehat{T}_n}}.$$

and its derivatives at the point $\widehat{T}_n$ are

(46)

$$\Psi'_{n-2}\left(\widehat{T}_n\right) = \frac{(n-1)(\widehat{T}_n^2+\widehat{T}_n-2)+2}{\widehat{T}_n^2-4}\Psi_n\left(\widehat{T}_n\right),$$

$$\Psi'_{n-1}\left(\widehat{T}_n\right) = \frac{2n-2+n\widehat{T}_n}{\widehat{T}_n^2-4}\Psi_n\left(\widehat{T}_n\right),$$

$$\Psi'_n\left(\widehat{T}_n\right) = \frac{2n+(n-1)\widehat{T}_n}{\widehat{T}_n^2-4}\Psi_n\left(\widehat{T}_n\right),$$

$$\Psi'_{n+1}\left(\widehat{T}_n\right) = \frac{n(\widehat{T}_n^2+\widehat{T}_n-2)-2}{\widehat{T}_n^2-4}\Psi_n\left(\widehat{T}_p\right).$$

Proof. We start by considering the equality,

$$A^{2n-1}(\hat{T}_n) = A^{n-1}(\widehat{T}_n)A^n(\widehat{T}_n) = I.$$

Then from (15), by dropping the functional dependence, we get

$$\begin{array}{cc} \Psi_n\Psi_{n+1} - \Psi_{n-1}\Psi_n = 1, & \Psi_{n-1}^2 - \Psi_n^2 = 0, \\ \Psi_{n-1}\Psi_{n+1} - \Psi_{n-2}\Psi_n = 0, & \Psi_{n-2}\Psi_{n-1} - \Psi_{n-1}\Psi_n = 1, \end{array}$$

and by resolving the above equations we obtain 45.

Finally, from Lemma A.4, we compute the derivatives (46).

□